Highlights from the CALET observations for 7.5 years on the International Space Station

ICRC2023
38th International Cosmic Ray Conference
The Astroparticle Physics Conference

Highlight Talk 2-01 - CRD

CALET

Calorimetric Electron Telescope

Shoji Torii
Waseda University, Japan
for the CALET Collaboration

July 26 -- August 3, 2023 The 38 th International Cosmic Ray Conference Nagoya, Japan

The CALET Collaboration Member

O. Adriani,[1,2] Y. Akaike,[3,4] K. Asano,[5] Y. Asaoka,[5] E. Berti,[2,13] G. Bigongiari,[6,7] W.R. Binns,[8] M. Bongi,[1,2] P. Brogi,[6,7] A. Bruno,[9] N. Cannady,[10,11,12] G. Castellini,[13] C. Checchia,[6,7] M.L. Cherry,[14] G. Collazuol,[15,16] G.A. de Nolfo,[9] K. Ebisawa,[17] A. W. Ficklin,[14] H. Fuke,[17] S. Gonzi,[1,2,13] T.G. Guzik,[14] T. Hams,[10] K. Hibino,[18] M. Ichimura,[19] K. Ioka,[20] W. Ishizaki,[5] M.H. Israel,[8] K. Kasahara,[21] J. Kataoka,[22] R. Kataoka,[23] Y. Katayose,[24] C. Kato,[25] N. Kawanaka,[20] Y. Kawakubo,[14] K. Kobayashi,[3,4] K. Kohri,[26] H.S. Krawczynski,[8] J.F. Krizmanic,[11] P. Maestro,[6,7] P.S. Marrocchesi,[6,7] A.M. Messineo,[7,27] J.W. Mitchell,[11] S. Miyake,[28] A.A. Moiseev,[11,12,29] M. Mori,[30] N. Mori,[2] H.M. Motz,[31] K. Munakata,[25] S. Nakahira,[17] J. Nishimura,[17] S. Okuno,[18] J.F. Ormes,[32] S. Ozawa,[33] L. Pacini,[2,13] P. Papini,[2] B.F. Rauch,[8] S.B. Ricciarini,[2,13] K. Sakai,[10,11,12] T. Sakamoto,[34] M. Sasaki,[11,12,29] Y. Shimizu,[18] A. Shiomi,[35] P. Spillantini,[1] F. Stolzi,[6,7] S. Sugita,[34] A. Sulaj,[6,7] M. Takita,[5] T. Tamura,[18] T. Terasawa,[5] S. Torii,[3] Y. Tsunesada,[36,37] Y. Uchihori,[38] E. Vannuccini,[2] J.P. Wefel,[14] K. Yamaoka,[39] S. Yanagita,[40] A. Yoshida,[33] K. Yoshida,[21] and W. V. Zober[8]

PI : Japan Co-PI : Italy Co-PI : USA

1) University of Florence, Italy
2) INFN Florence, Italy
3) WISE, Waseda University, Japan
4) JEM Utilization Center, JAXA, Japan
5) ICRR, University of Tokyo, Japan
6) University of Siena, Italy
7) INFN Pisa, Italy
8) Washington University, St. Louis, USA
9) Heliospheric Physics Laboratory, NASA/GSFC, USA
10) University of Maryland, Baltimore County, USA
11) Astroparticle Physics Laboratory, NASA/GSFC, USA
12) CRESST, NASA/GSFC, USA
13) IFAC, CNR, Italy
14) Louisiana State University, USA
15) University of Padova, Italy
16) INFN Padova, Italy
17) ISAS, JAXA, Japan
18) Kanagawa University, Japan
19) Hirosaki University, Japan
20) YITP, Kyoto University, Japan
21) Shibaura Institute of Technology, Japan
22) ASE, Waseda University, Japan
23) NIPR, Japan
24) Yokohama National University, Japan
25) Shinshu University, Japan
26) IPNS, KEK, Japan
27) University of Pisa
28) NIT(KOSEN), Ibaraki College, Japan
29) University of Maryland, College Park, USA
30) Ritsumeikan University, Japan
31) GCSE, Waseda University, Japan
32) University of Denver, USA
33) NICT, Japan
34) Aoyama Gakuin University, Japan
35) Nihon University, Japan
36) Osaka Metropolitan University, Japan
37) NITEP, Osaka Metropolitan University, Japan
38) QST, Japan
39) Nagoya University, Japan
40) Ibaraki University, Japan

Guest Investigator: Lauren W. Blum (University of Colorado Boulder, USA), M. Teramoto (Kyushu Institute of Technology, Japan)

CALET Payload

Kounotori (HTV) 5

Launched on Aug. 19th, 2015 by the Japanese H2-B rocket

Emplaced on JEM-EF port #9 on Aug. 25th, 2015

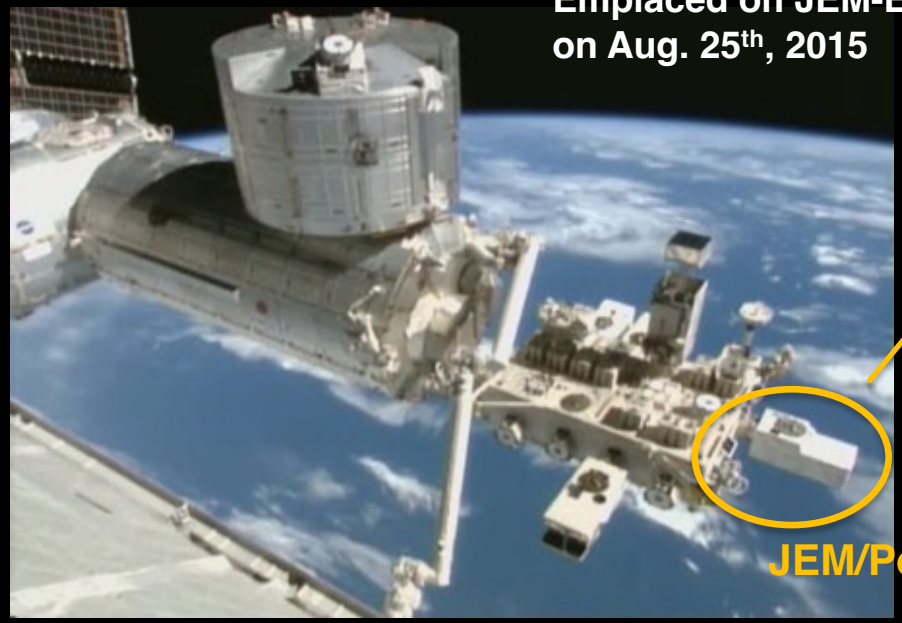

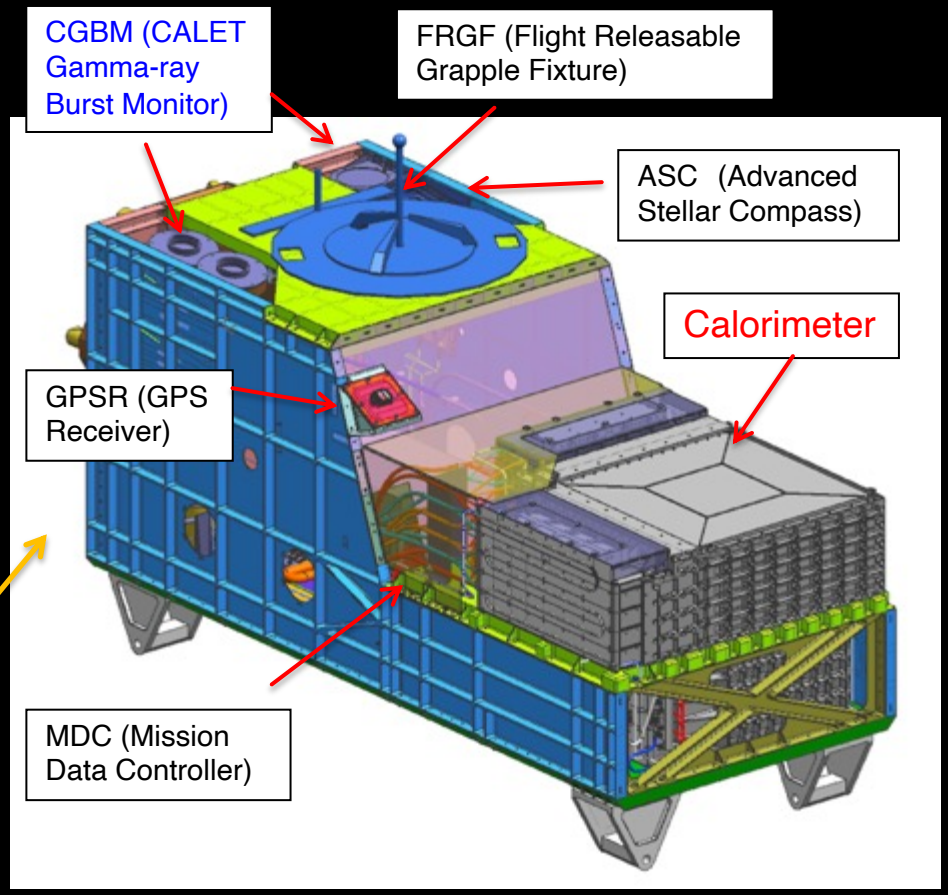

- **Mass: 612.8 kg**
- **JEM Standard Payload Size:**
  1850mm(L) × 800mm(W) × 1000mm(H)
- **Power Consumption: 507 W（max）**
- **Telemetry:**
  Medium 600 kbps (6.5GB/day) / Low 50 kbps

Overview of the CALET Calorimeter

Field of view: ~ 45 degrees (from the zenith) : Geometrical Factor: ~ 1,040 cm^{2}sr (for electrons) : Thickness: 30 X_0, 1.3 λ_I

CHD/IMC

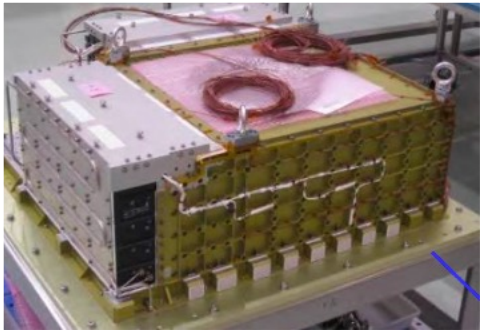

TASC

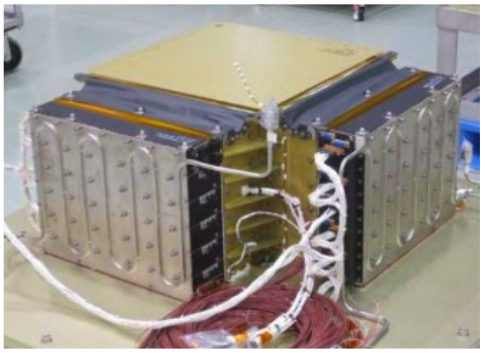

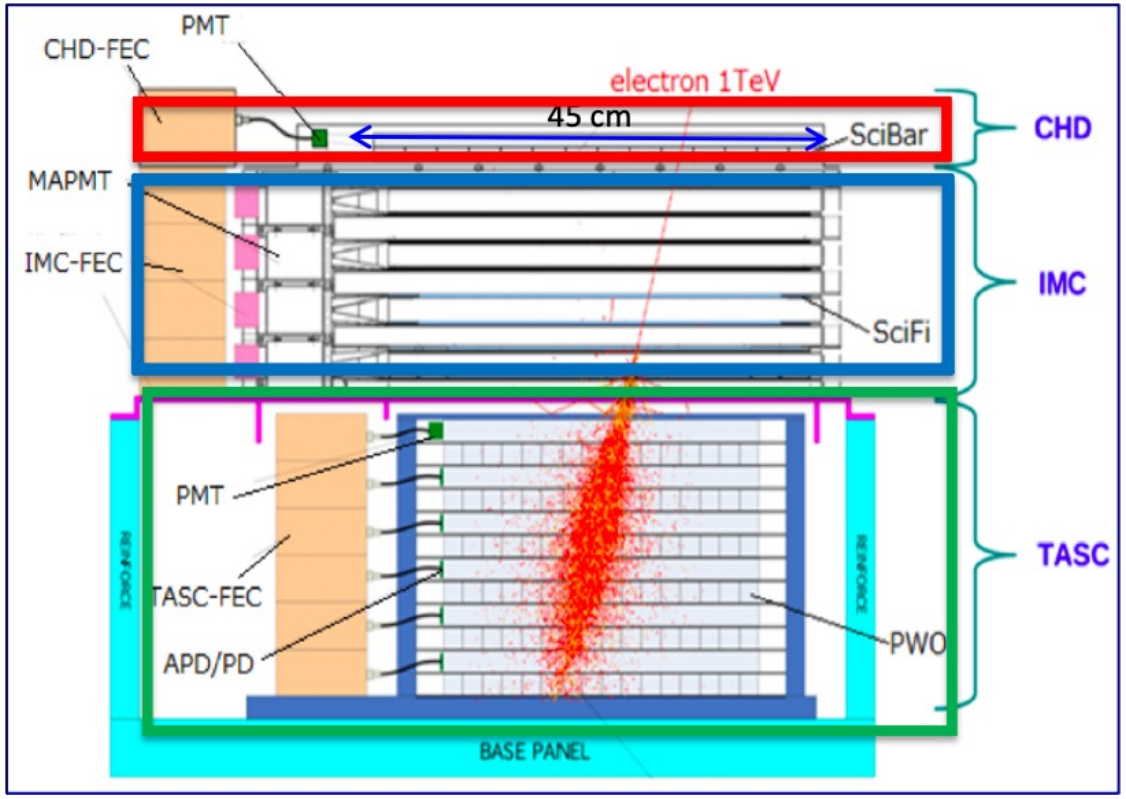

CHD – Charge Detector

- 2 layers x 14 plastic scintillating paddles
- **single element charge ID** from p to Fe and above (Z = 40)
- charge resolution ~0.1-0.3 e

IMC – Imaging Calorimeter

- Scifi. + tungsten absorbers: **3 X_0**
- 8 x 2 x 448 plastic scintillating fibers (1mm) **readout individually**
- **tracking** (~0.1° angular resolution) + **Shower imaging**

TASC – Total Absorption Calorimeter

- 6 x 2 x 16 lead tungstate ($PbWO_4$) logs: **27 X_0, 1.2 λ_I**
- **energy resolution:** ~2 % (>10GeV) for e , γ ~30-35% for p, nuclei
- **e/p separation:** ~10^{-5}
- **angular resolution:** 0.2° for gamma-rays > ~50 GeV

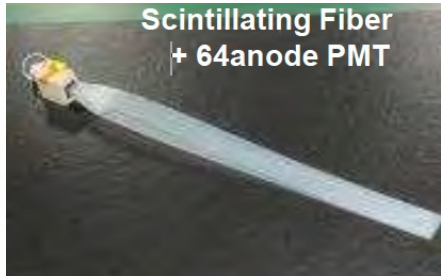

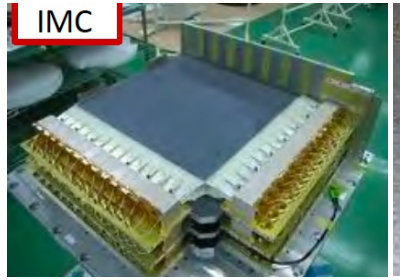

Examples of CALET Event Candidates

Electron, E=3.05 TeV

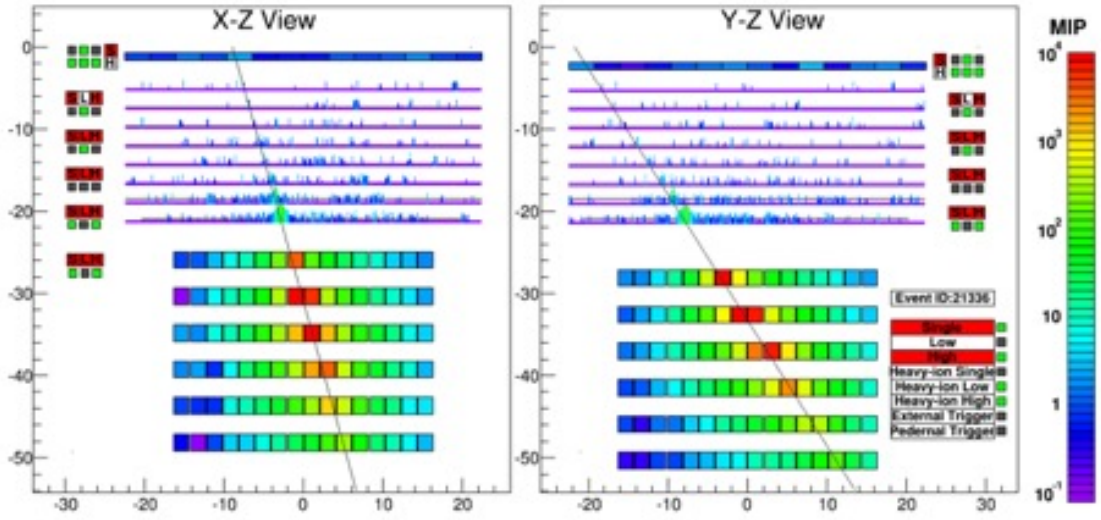

Proton, E_{TASC}=2.89 TeV

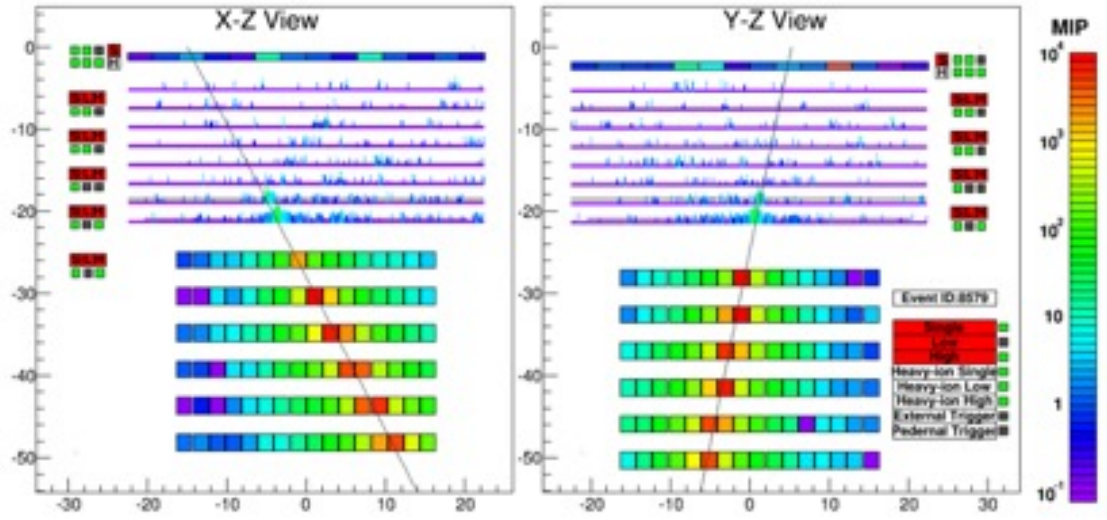

Gamma-ray, E=44.3 GeV

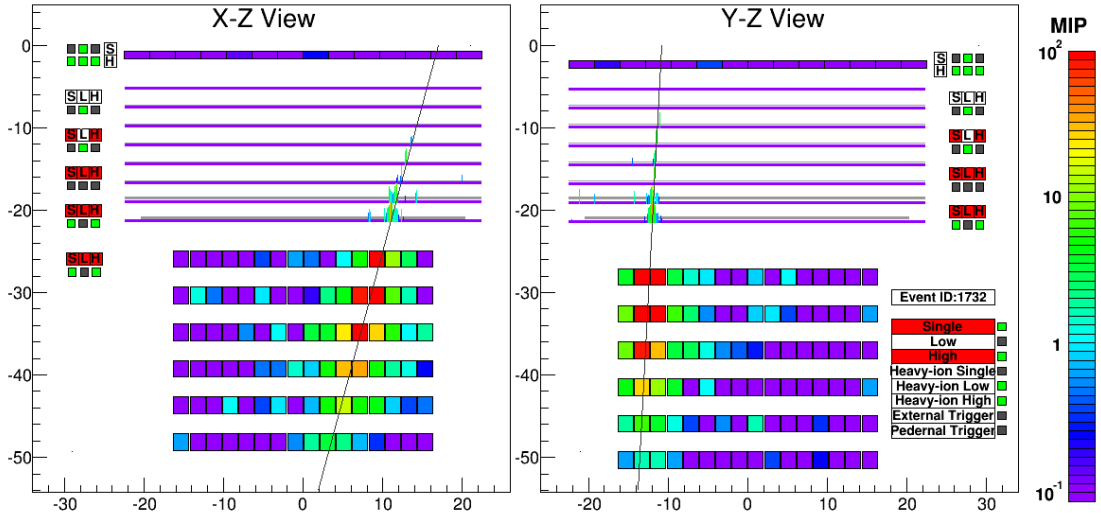

Iron, E_{TASC} =9.3 TeV

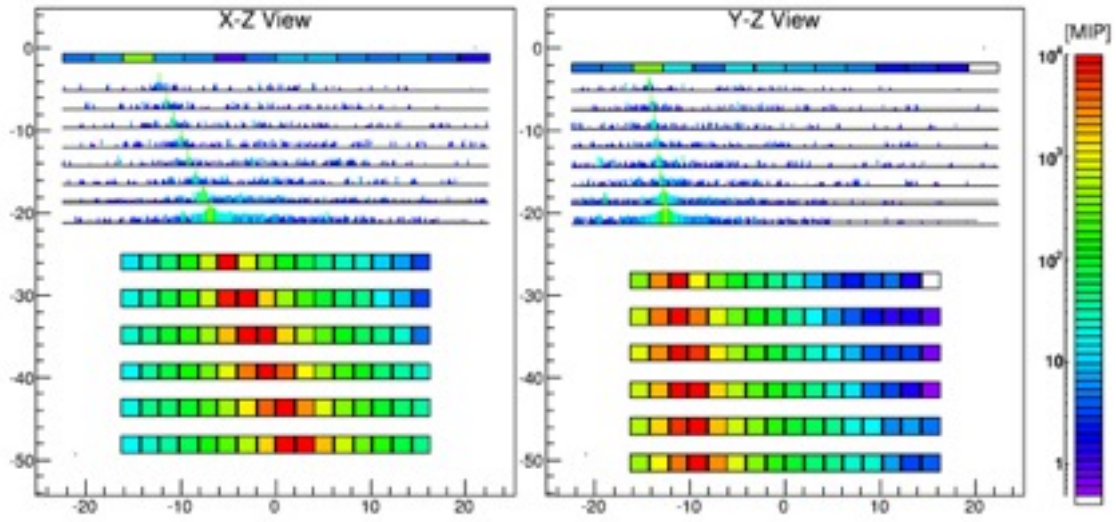

Energy Measurement: a wide dynamic range 1-10^6 MIPs

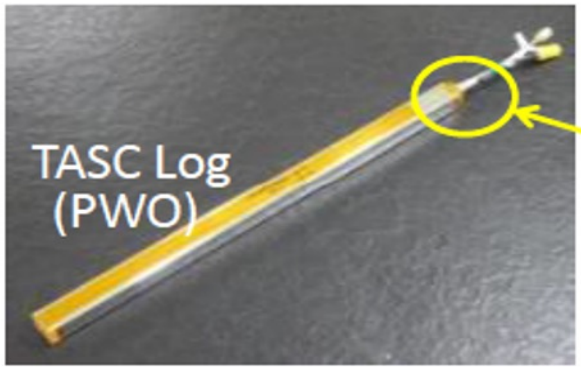

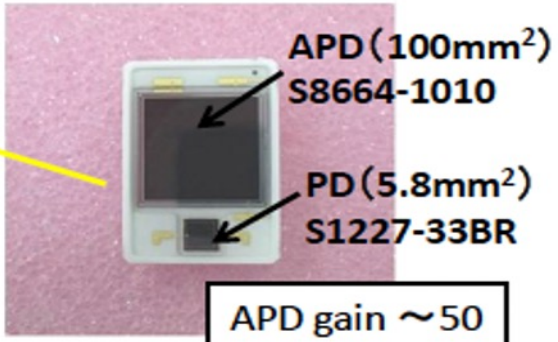

"MIP" peak in PWO: Obs. vs. MC

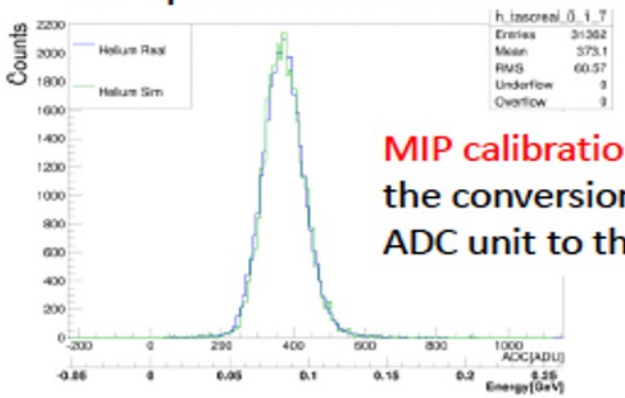

MIP calibration determines the conversion factor from ADC unit to the energy

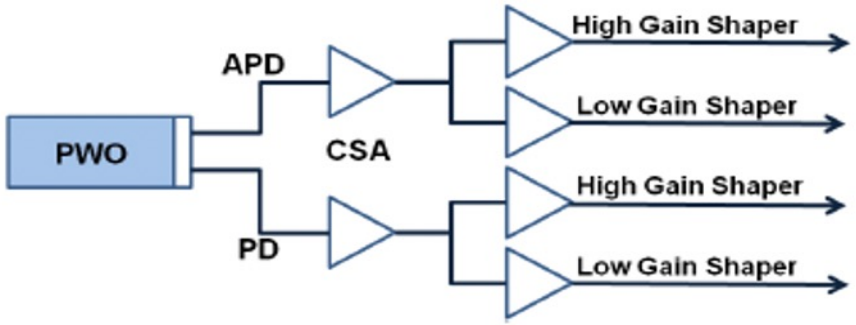

The whole dynamic range was calibrated by UV laser irradiation on ground :
1) The linearity of each gain range is confirmed in the range of 1.4-2.5 %.
2) Each channel covers from 1 MIP to 10^6 MIPs.

APD-H	APD-L	PD-H	PD-L
1.4%	1.5%	2.5%	2.2%

The correlation between adjacent gain ranges is calibrated by using in-flight data in each channel.

APD-H APD-L	APD-L PD-H	PD-H PD-L
0.1%	0.7%	0.1%

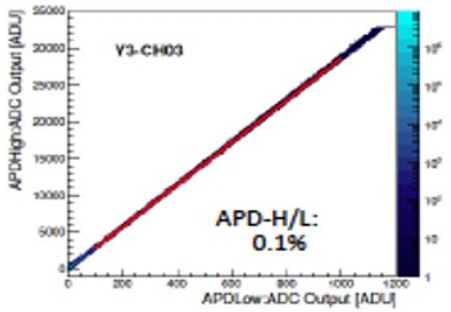

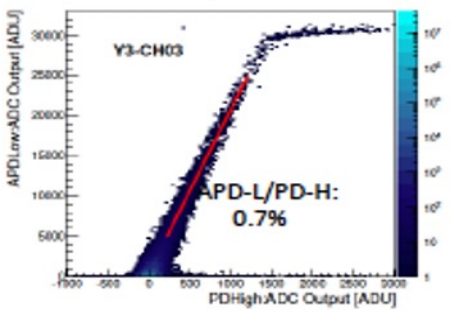

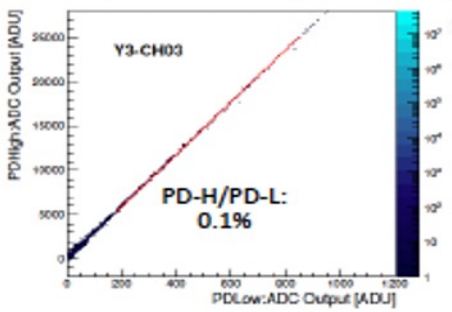

Example of energy distribution in one PWO log

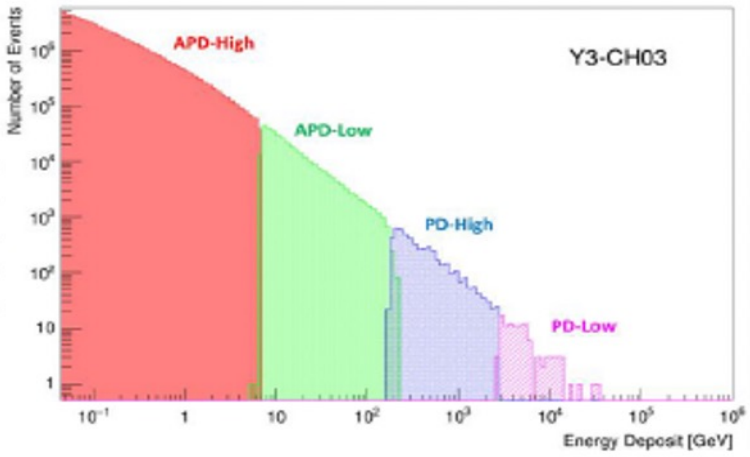

Energy Measurement: energy scale and resolution

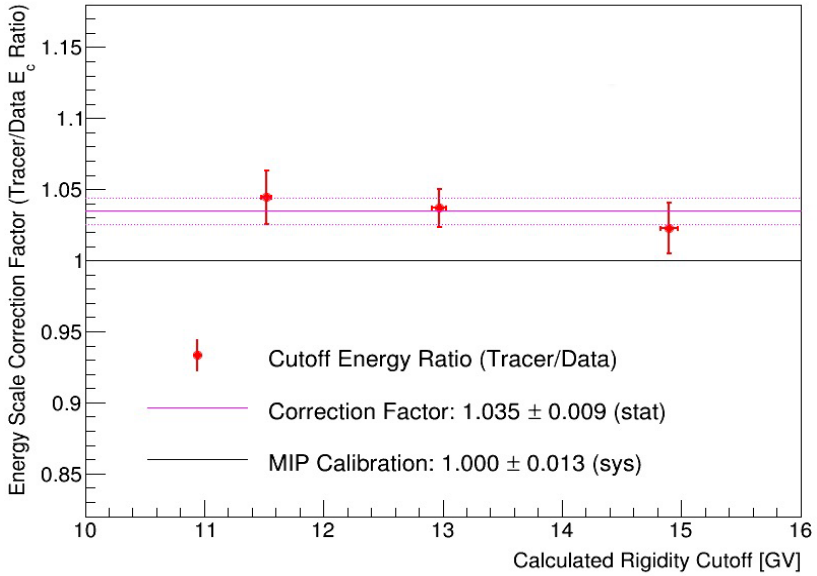

ELECTRONS

Absolute energy scale calibration for electrons using rigidity cutoff + beam calibration at CERN-SPS

Simulated energy dependence of electron energy resolution:
< 2% above 20 GeV
using both TASC and IMC
Including the calibration errors

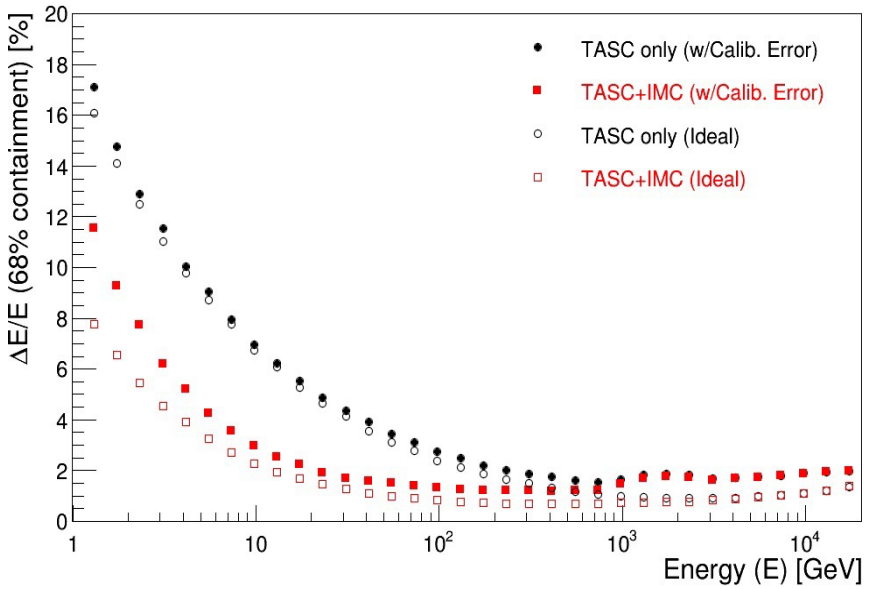

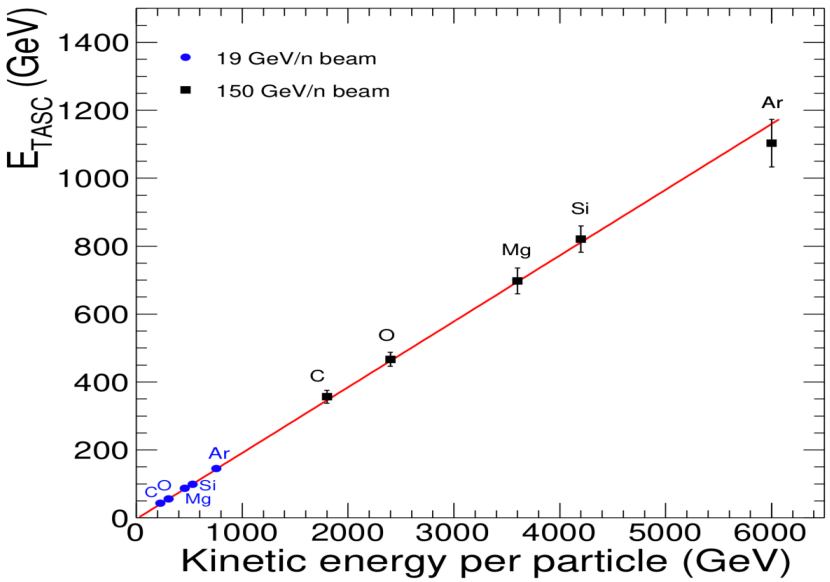

HADRONS

Beam calibration at CERN-SPS with Ion fragments at 13, 19 150 GeV/n

Linearity assessed up to ~6 TeV with primary beam of 40Ar at 150 GeV/n

Energy resolution ~30%

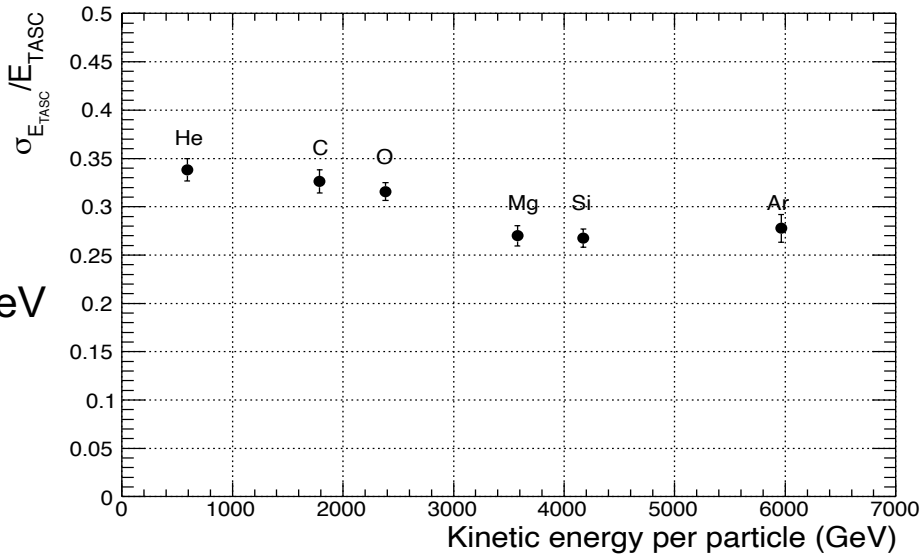

CALET Orbital Operations (during the first 7.5 years)

PCRD0-13

Geometrical Factor:
- 1040 cm^2 sr for electrons, light nuclei
- 1000 cm^2 sr for gamma-rays
- 4000 cm^2sr for ultra-heavy nuclei

High-energy trigger (> 10 GeV) statistics:
- Orbital operations : **2818 days (>7.5 years)** as of June 30, 2023
- Observation time : 2.39×10^8 sec
- Live time fraction: ~ **86%**
- Exposure of HE trigger : **~250 m^2 sr day**

Time duration of observation (day by day)

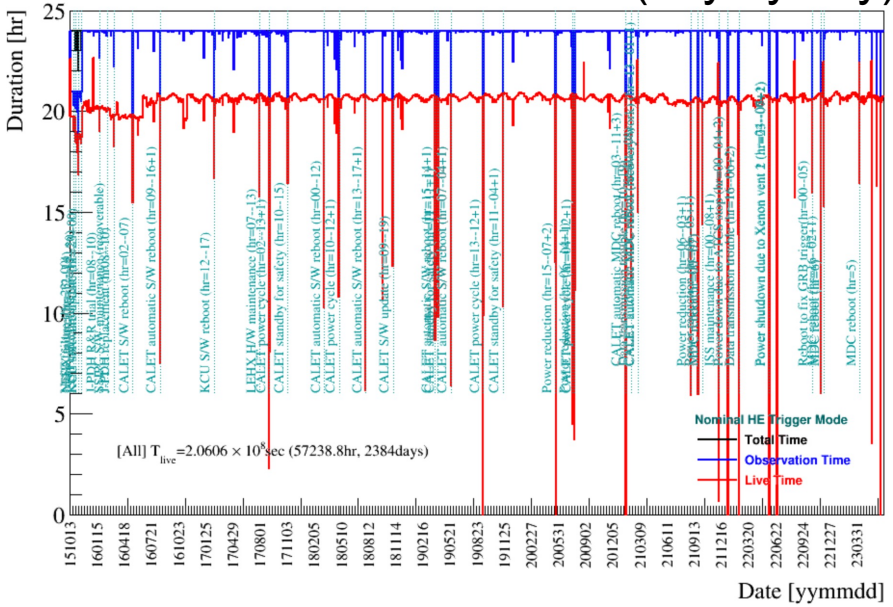

20.6 hours per day on average

Energy deposit (in TASC) spectrum: 1 GeV-1 PeV

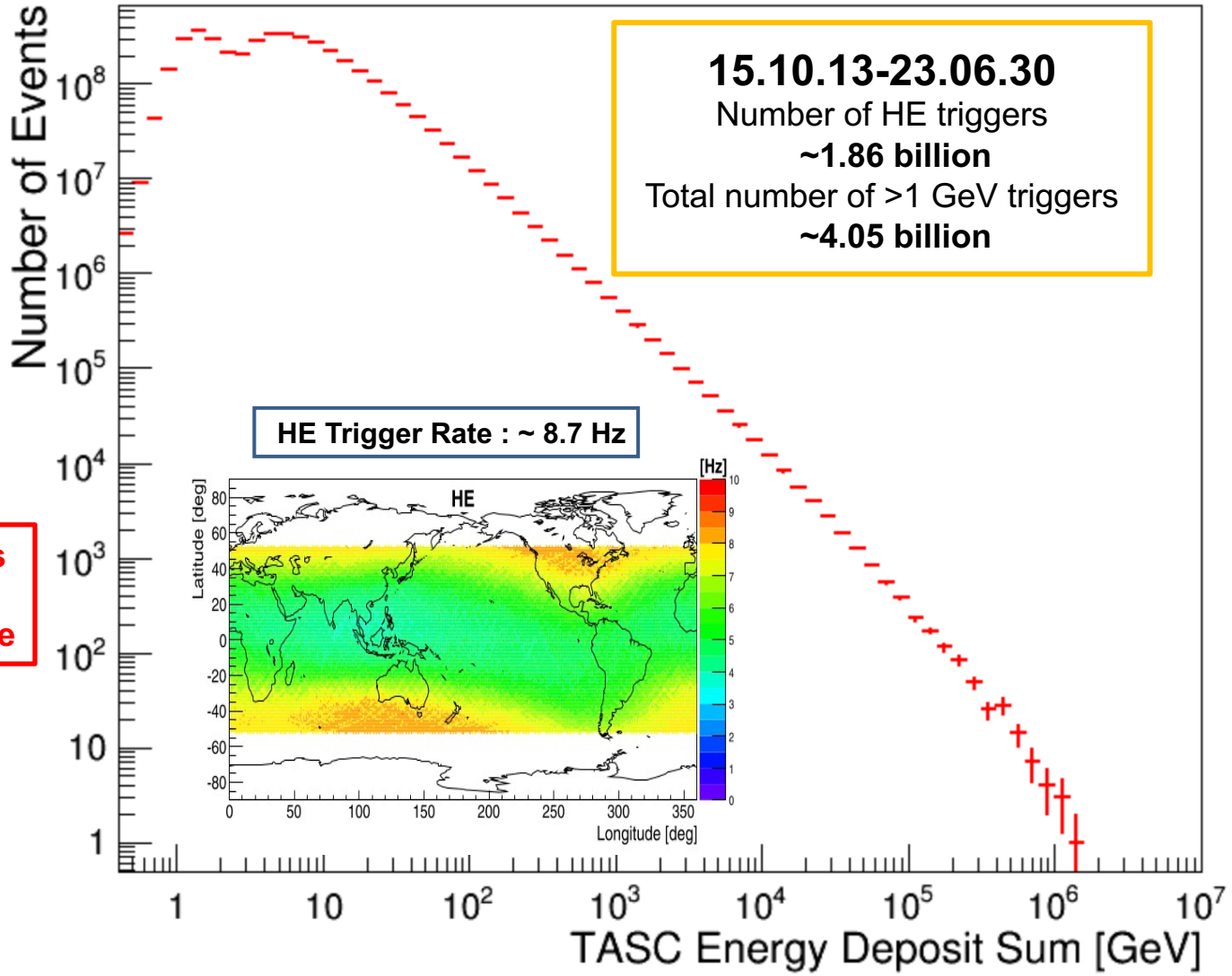

Cosmic-ray All-electron Spectrum up to 7.5 TeV

CRD5-02

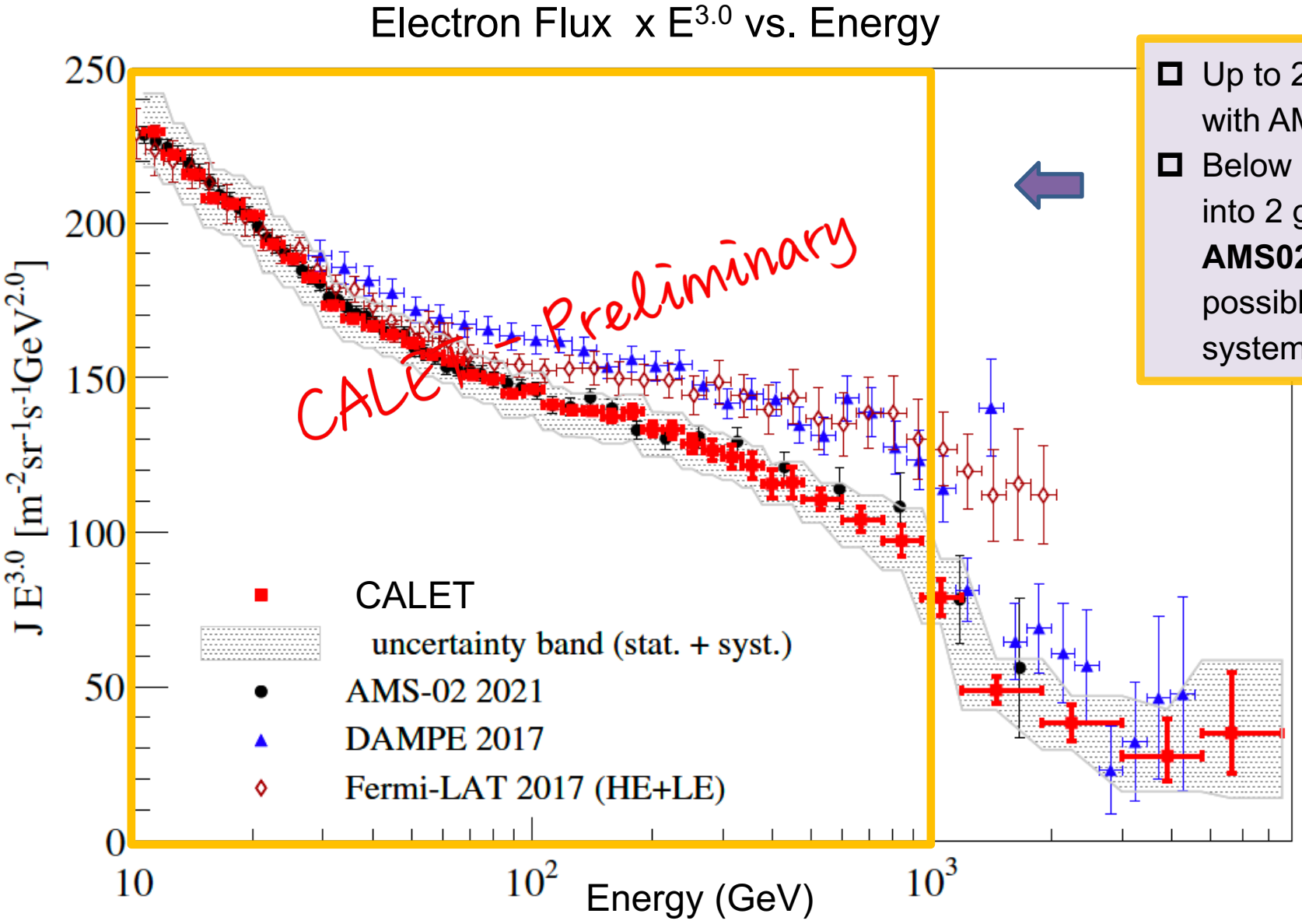

- Up to 2 TeV : CALET spectrum is consistent with AMS-02
- Below 1 TeV : Present measurements cluster into 2 groups:
  AMS02 + CALET and **FERMI + DAMPE**
  possibly indicating the presence of unkown systematics

Preliminary spectrum is **updated** using 2637 days of CALET observations:
Oct.13, 2015 – Dec. 31, 2022
7.02 million events > 10 GeV

DM5-03 PCRD2-07

Interpretation of the spectrum by Dark Matter and Astrophysical Sources

Cosmic-ray All-electron Spectrum up to 7.5 TeV

CRD5-02

Electron Flux x $E^{3.0}$ vs. Energy

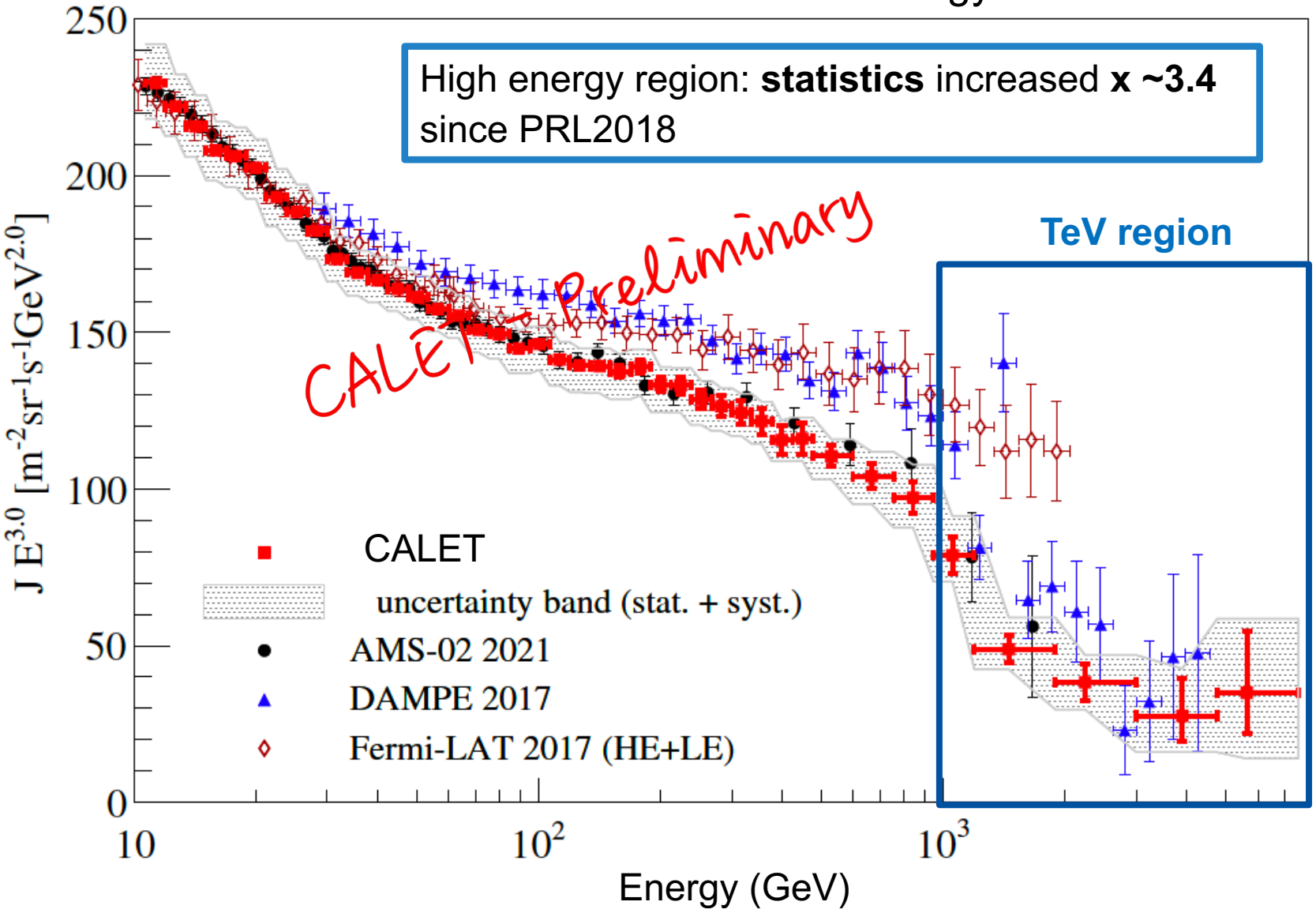

Energy loss due to Synchrotron and Inverse Compton : $dE/dt = -bE^2$

⇨ Observable sources of the electrons in the TeV region should be located at a distance < ~1 kpc and produced at a year < ~10^5 yr.

⇨ **Softening of the spectrum is expected above 1 TeV** since only a few SNRs are observed to keep this condition.

CALET observes a flux suppression above 1 TeV with a **significance > 6 σ**, a considerable improvement with respect to the result published in PRL2018 (~4 σ).

PCRD2-13 PCRD3-06

Advanced analysis is going on for electron identification above 5 TeV.

Cosmic-ray Proton Spectrum

PRL 129 101102 (2022) + CRD1-01

Flux x $E^{2.7}$ vs. Kinetic energy [Oct.2015- Apr.2023]

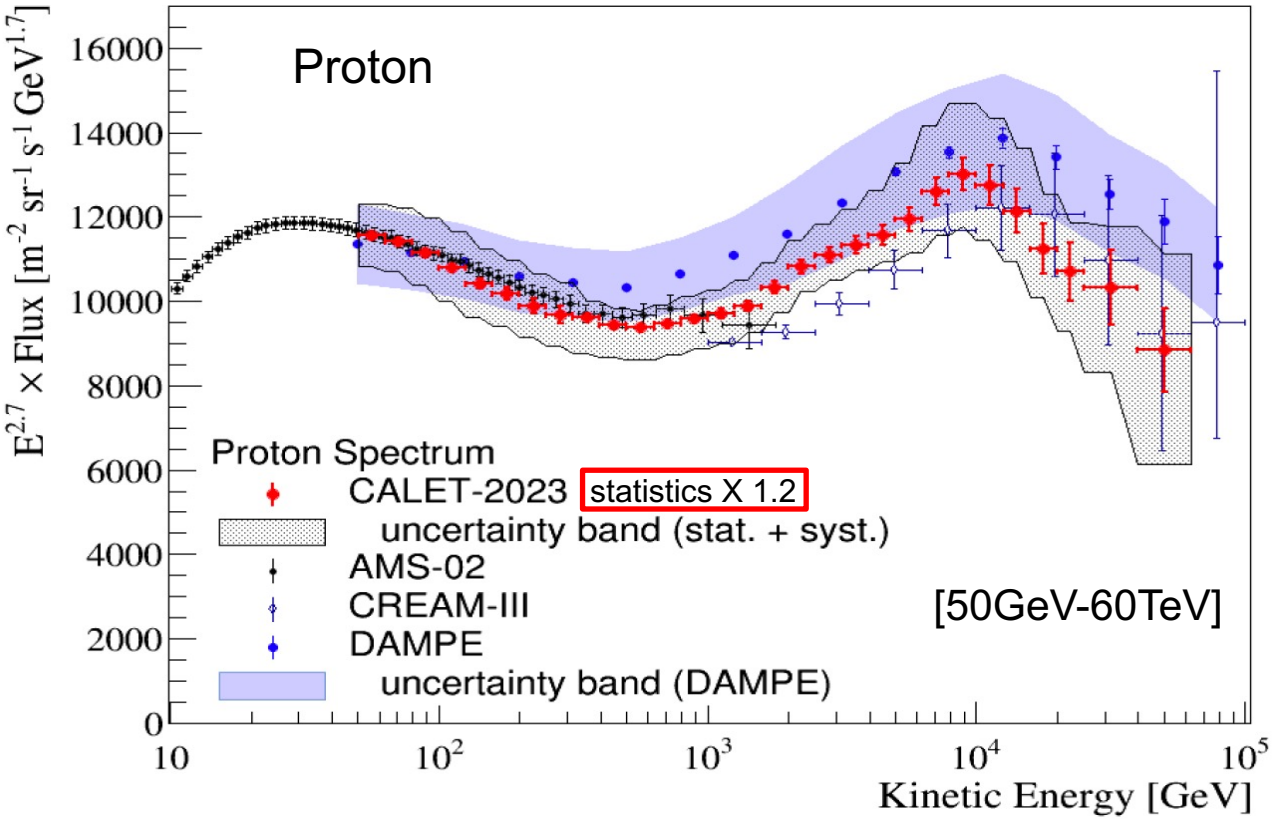

Fitting by DBPL Function

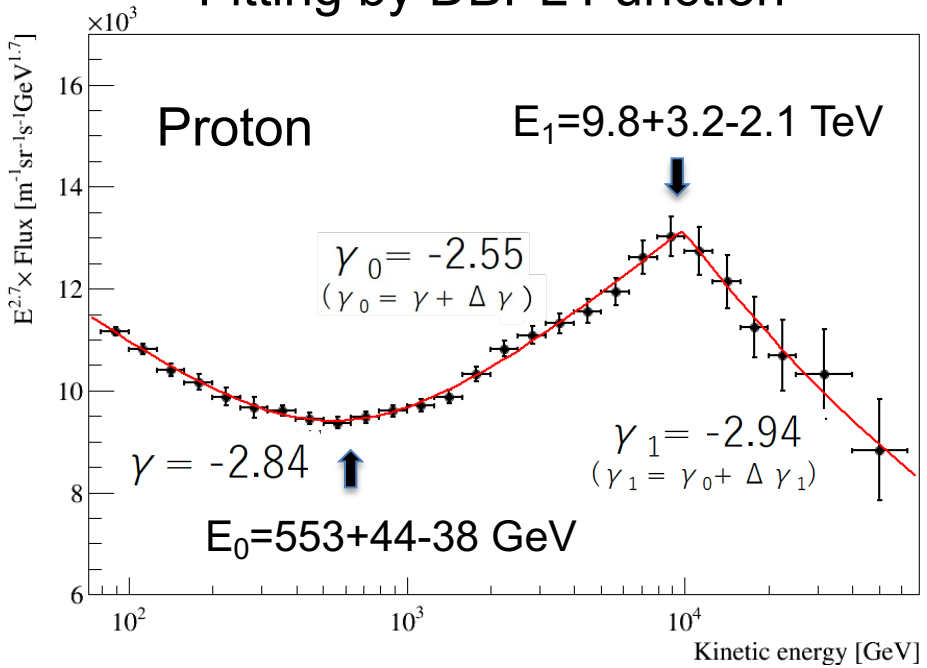

Energy dependence of power index

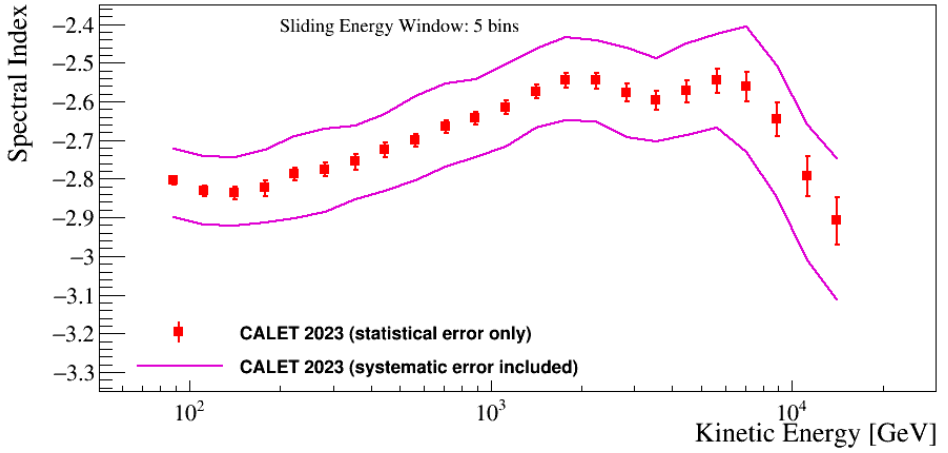

Double Power Law Function: HARDENING SOFTENING

$$\Phi(E) = C \times \left(\frac{E}{1\ \mathrm{GeV}}\right)^{\gamma} \times \left[1 + \left(\frac{E}{E_0}\right)^{s}\right]^{\frac{\Delta\gamma}{s}} \times \left[1 + \left(\frac{E}{E_1}\right)^{s_1}\right]^{\frac{\Delta\gamma_1}{s_1}}$$

Cosmic-ray Helium Spectrum

PRL 130 171002 (2023) + CRD1-02

Flux x $E^{2.6}$ vs. Kinetic energy [Oct. 2015 - Apr. 2022]

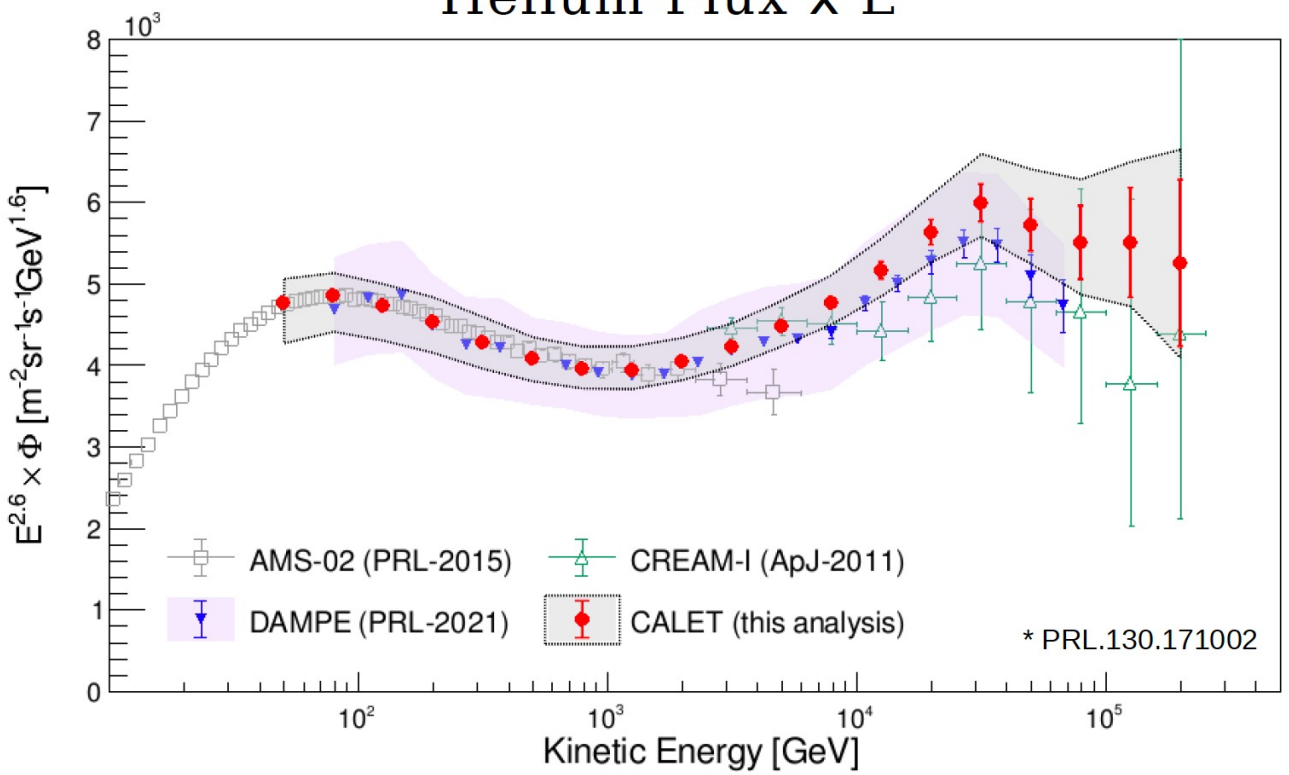

Fitting by Double Power Law (DBPL) function

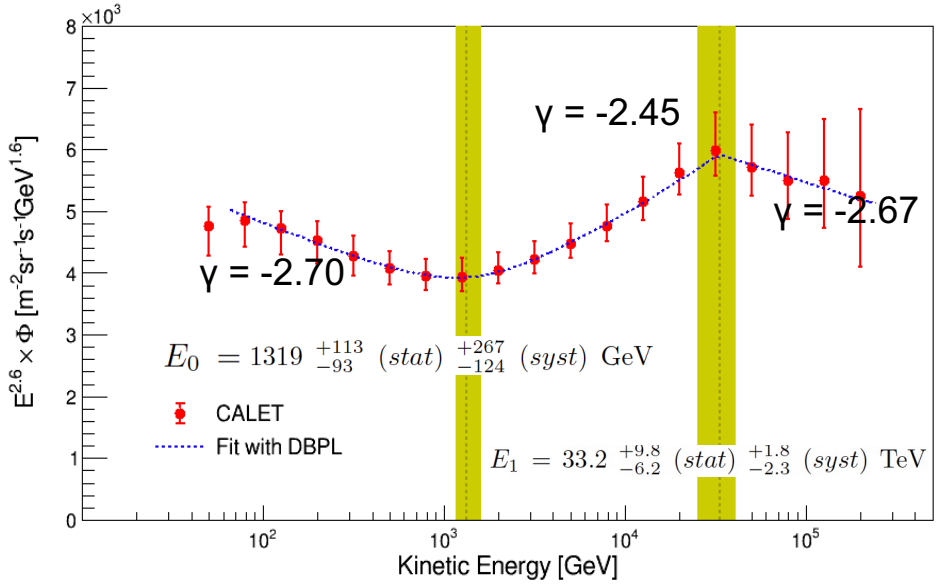

Energy dependence of power index

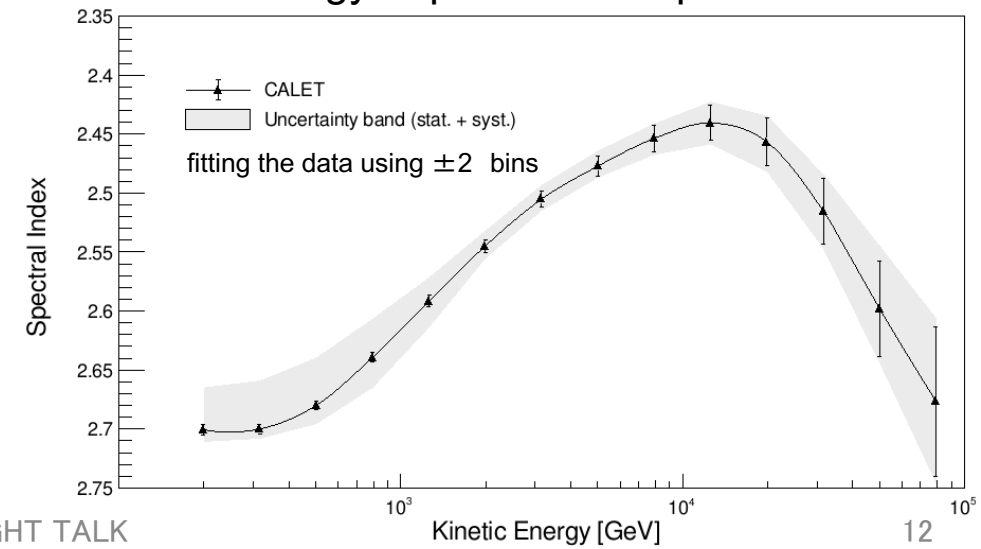

Double Power Law Function: HARDENING SOFTENING

$$\Phi(E) = C\left(\frac{E}{GeV}\right)^{\gamma}\left[1+\left(\frac{E}{E_0}\right)^{S}\right]^{\frac{\Delta\gamma}{S}}\left[1+\left(\frac{E}{E_1}\right)^{S_1}\right]^{\frac{\Delta\gamma_1}{S_1}}$$

Comparison of Proton and Helium Spectrum

PRL 130 171002 (2023) + CRD1-02

Proton & Helium Spectrum vs Energy/nucleon

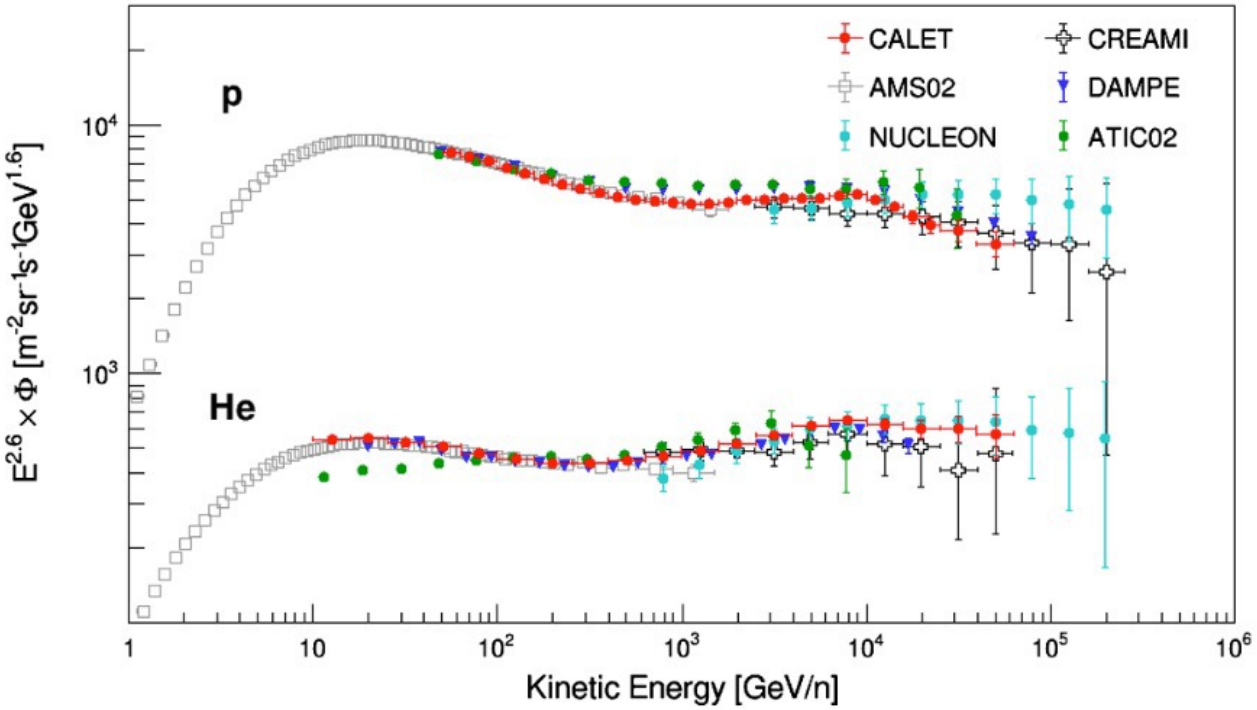

Proton & Helium Spectrum vs Rigidiy

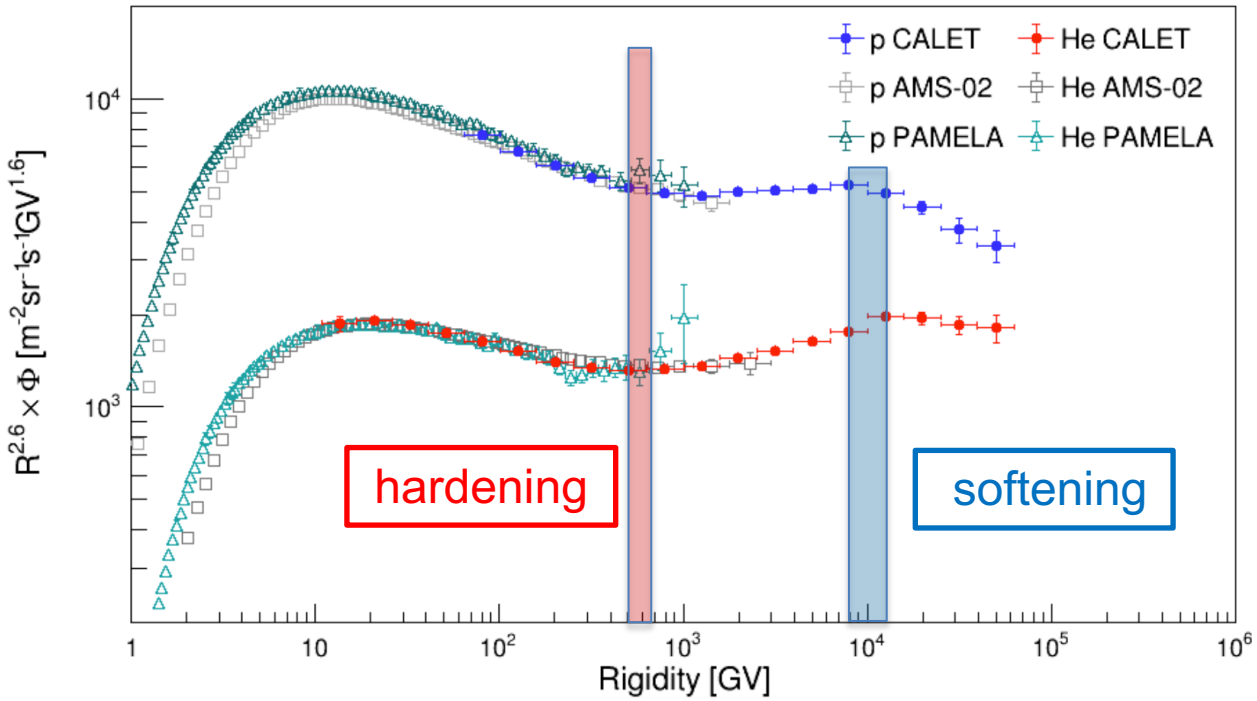

- Both of proton and helium spectrum have a similar structure of hardening and softening around same region of rigidities.
- The softening of p & He spectrum around 10 TV indicates a possible relation to the energy limit of shock wave acceleration in SNR.

Proton / Helium Ratio

PRL 130 171002 (2023) + CRD1-02

Proton/Helium Ratio vs. Energy/nucleon

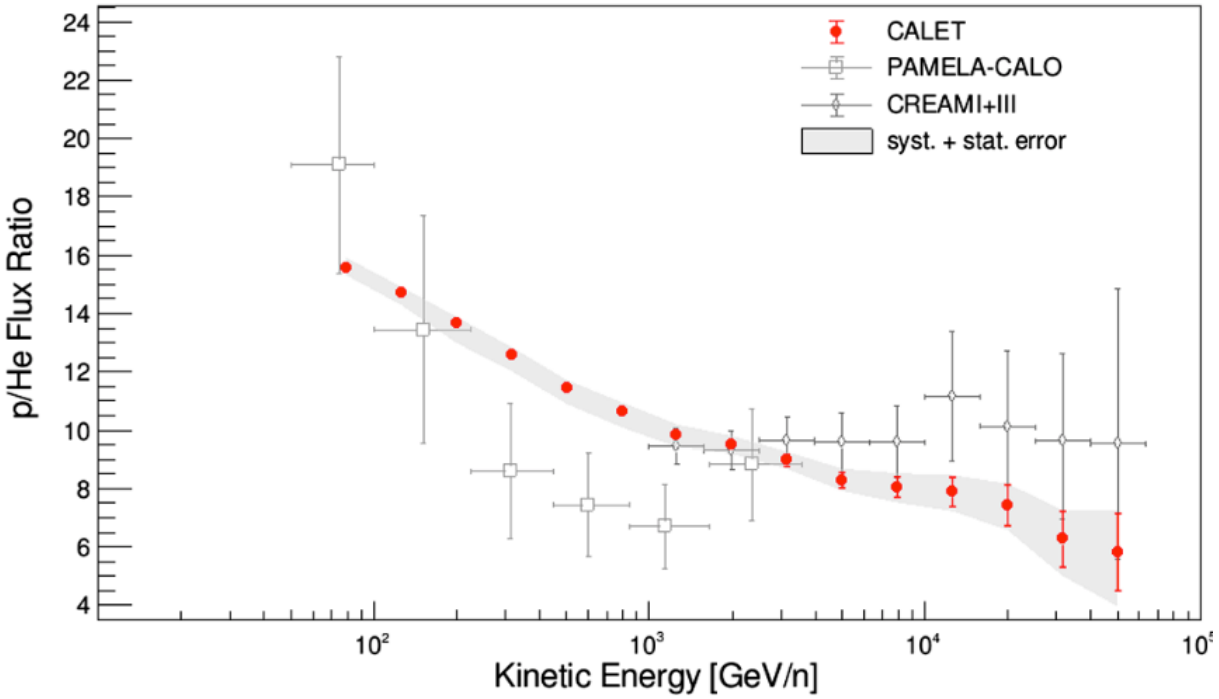

Proton/Helium Ratio vs. Rigidity

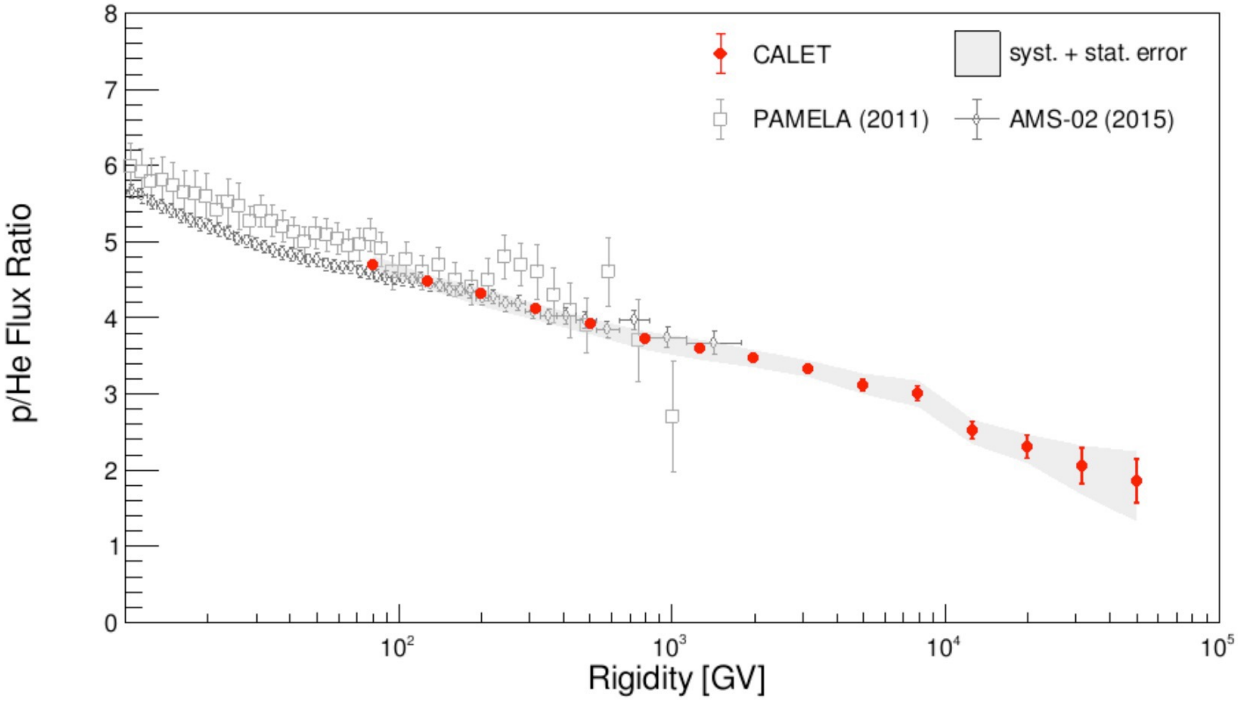

- The spectral index of helium is harder than that of proton (by ~0.1) in the whole rigidity range.
- Possible change of the spectral index of p/He ratio seen above 10 TV will be carefully checked by analyzing higher statistics data in future.

Nuclei Measurement: Charge Identification with CHD and IMC

Single element identification for p, He and light nuclei is achieved by CHD+IMC charge analysis.

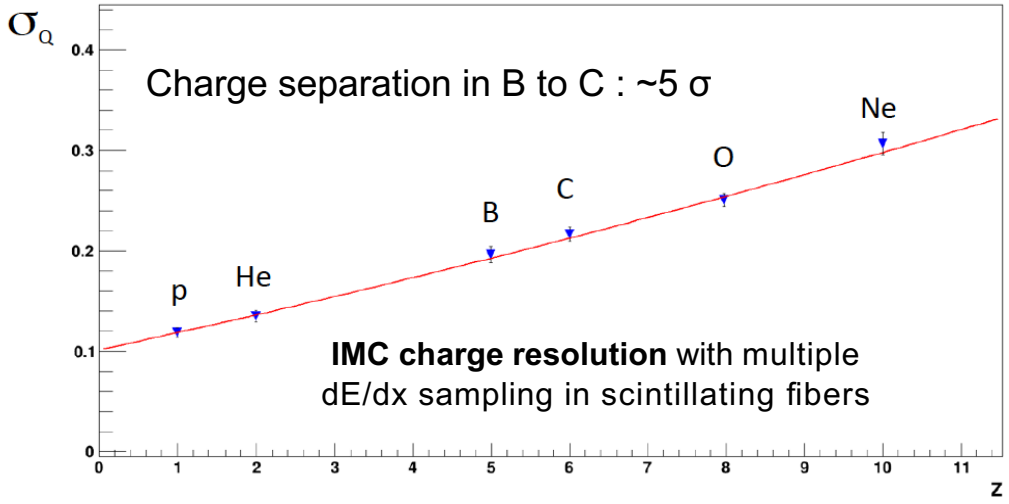

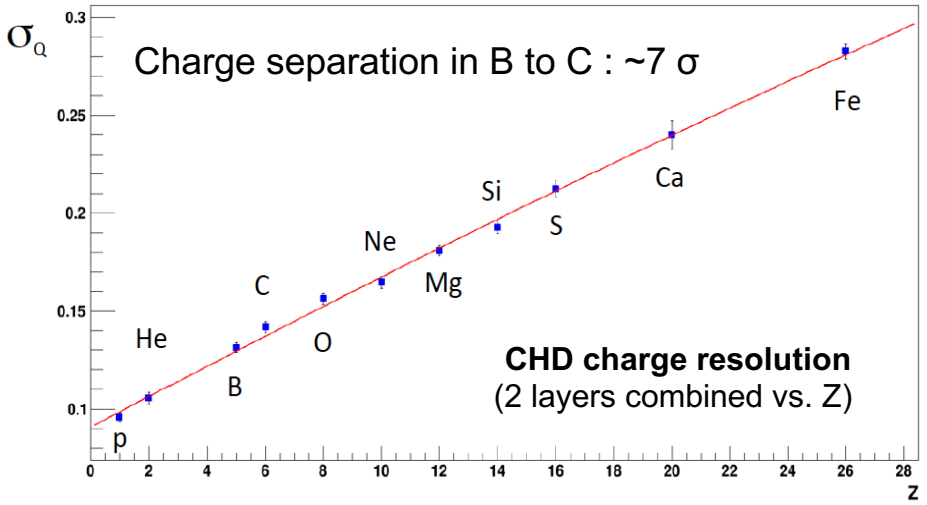

Low Energy

High Energy

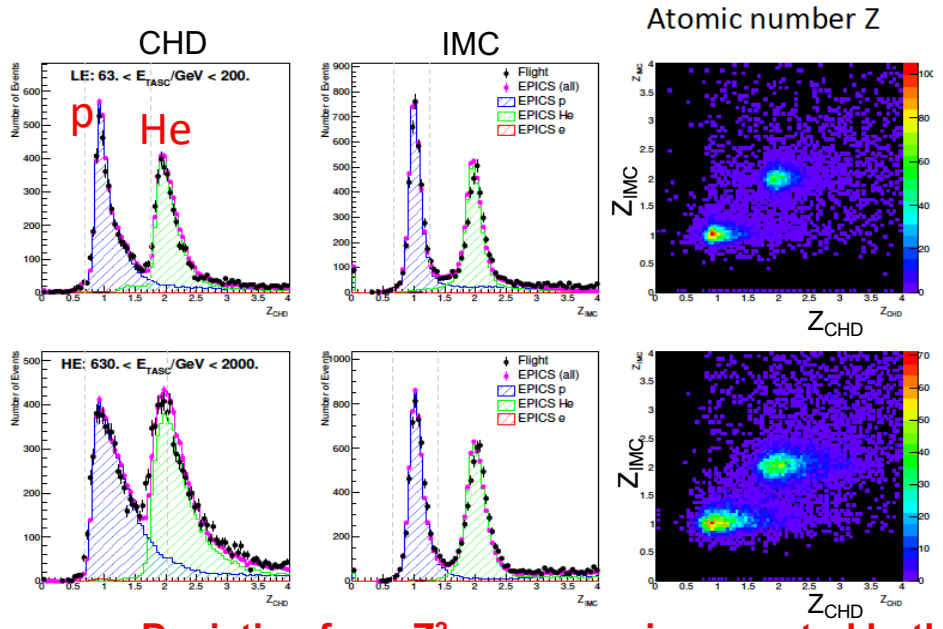

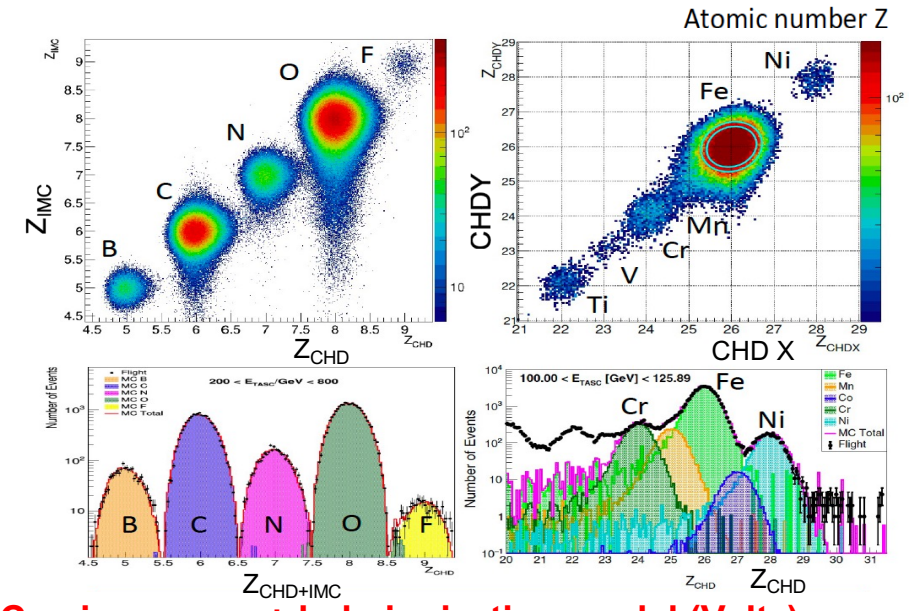

Deviation from Z^2 response is corrected both in CHD and IMC using a core + halo ionization model (Voltz)

Observations of Cosmic-ray Nuclei from C to Fe

Preliminary spectra of Carbon – Iron

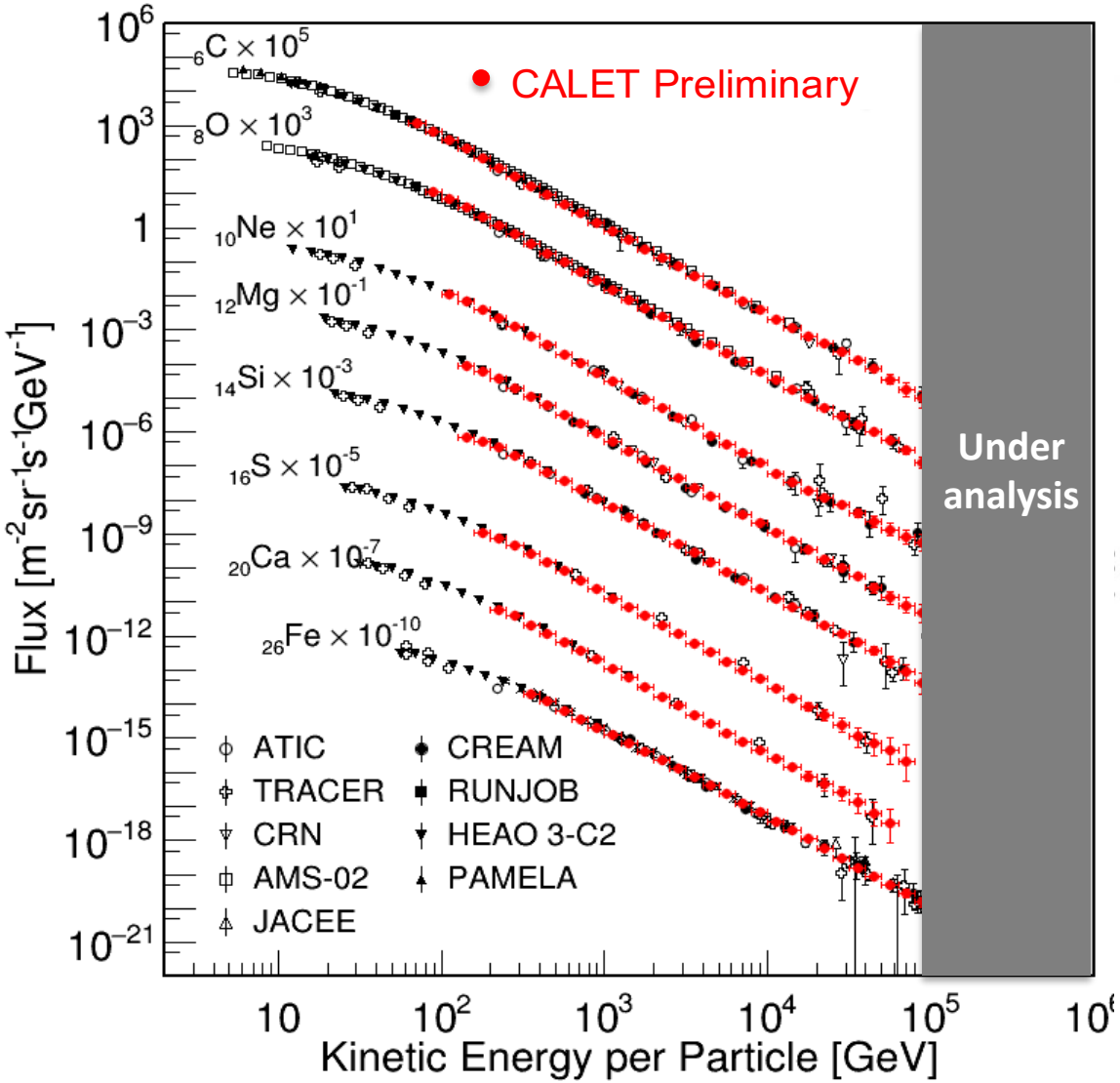

With excellent charge-ID of individual elements CALET is exploring the Table of Elements in the multi-TeV domain

Charge distribution from Proton to Nickel
(periodic table of elements by CALET)

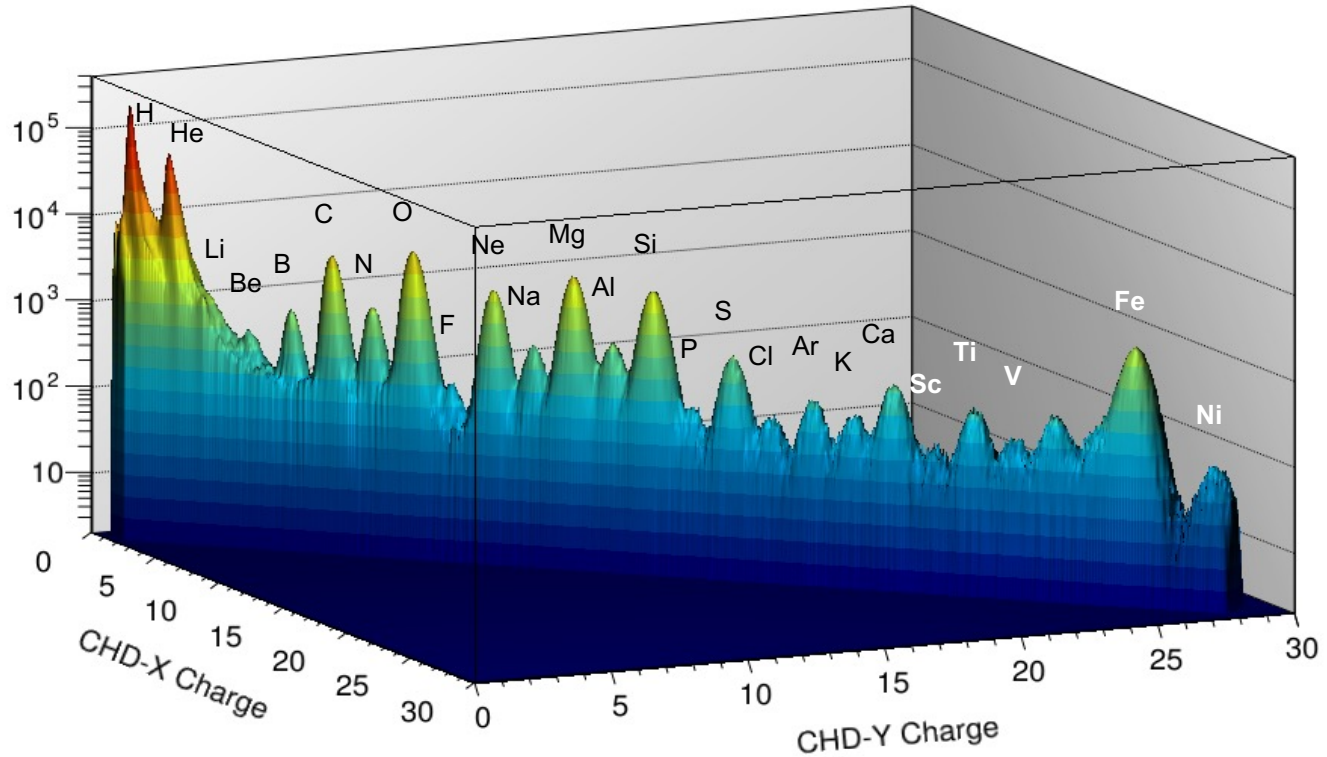

Carbon, Oxygen and Boron Energy Spectra

PRL 125 251102 (2020) + CRD4-04

Flux x $E^{2.7}$ vs kinetic energy per nucleon [8.4 GeV- 3.8 TeV]

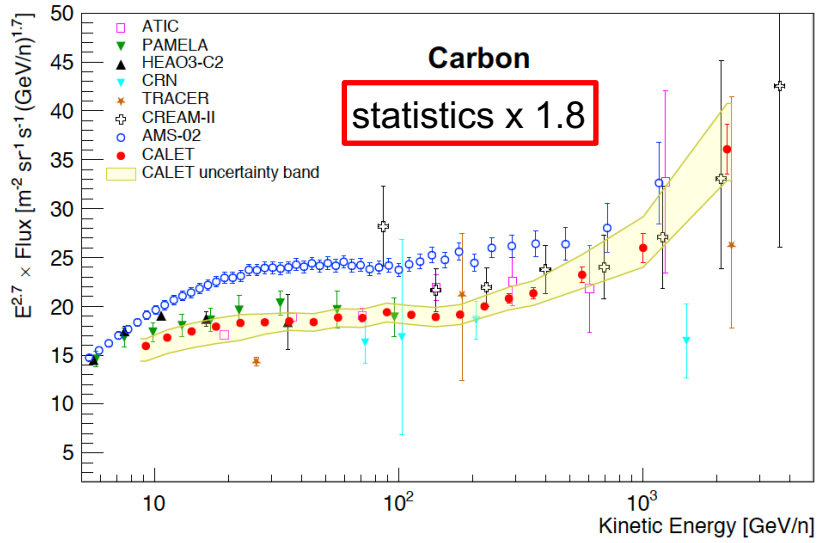

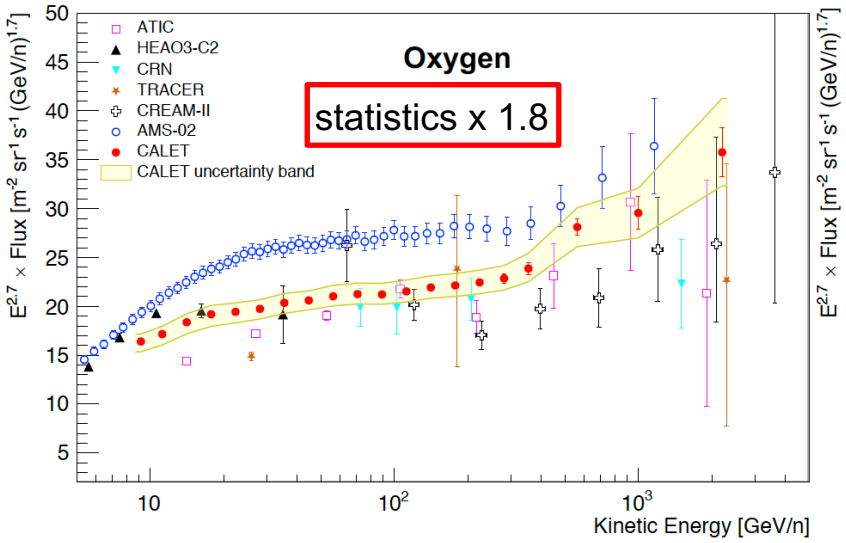

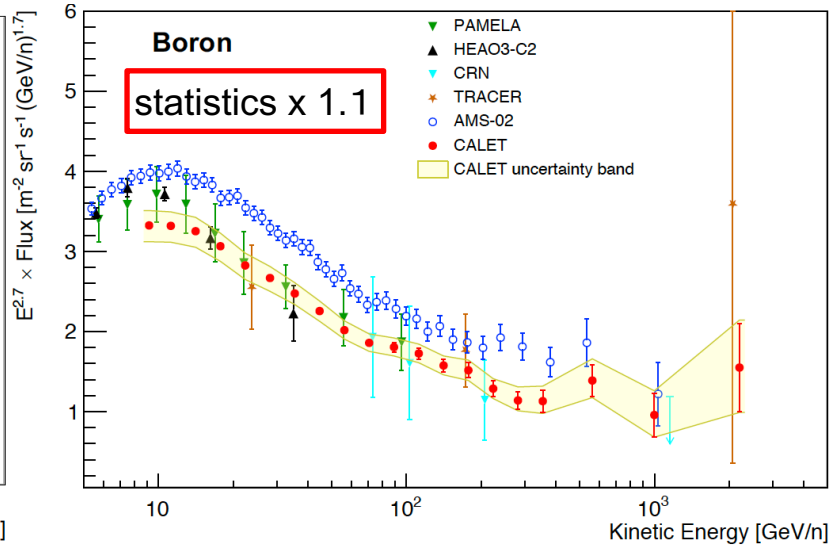

Fitting with double power law function

$$\Phi(E) = \begin{cases} c\left(\frac{E}{\mathrm{GeV}}\right)^{\gamma} & E \le E_0 \\ c\left(\frac{E}{\mathrm{GeV}}\right)^{\gamma}\left(\frac{E}{E_0}\right)^{\Delta\gamma} & E > E_0 \end{cases}$$

C-O fit
$\gamma = -2.66 \pm 0.02$
$E_0 = (260 \pm 50)$ GeV/n
$\Delta\gamma = 0.19 \pm 0.04$
χ^2/dof = 23/25

B fit
$\gamma = -3.03 \pm 0.03$
E_0 fixed from C-O
$\Delta\gamma = 0.32 \pm 0.14$
χ^2/dof = 5.2/11

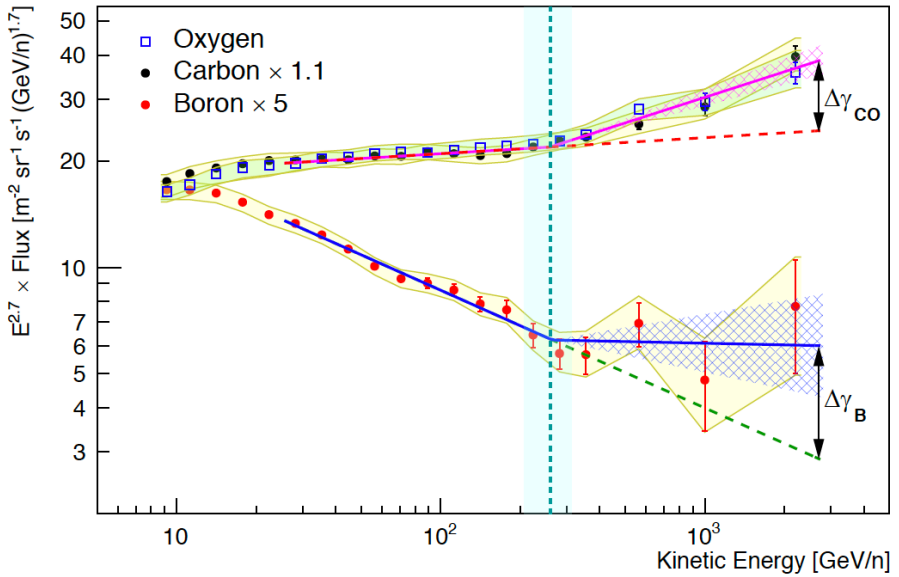

- C and O fluxes harden in a similar way above 200 GeV/n.
- B spectrum clearly different from C-O as expected for primary and secondary CR.
- The flux hardens more for B than for C and O above 200 GeV/n, albeit with low statistical significance.

B/C, B/O and C/O Flux Ratio

PRL 125 251102 (2020) + CRD4-04

B/C flux ratio

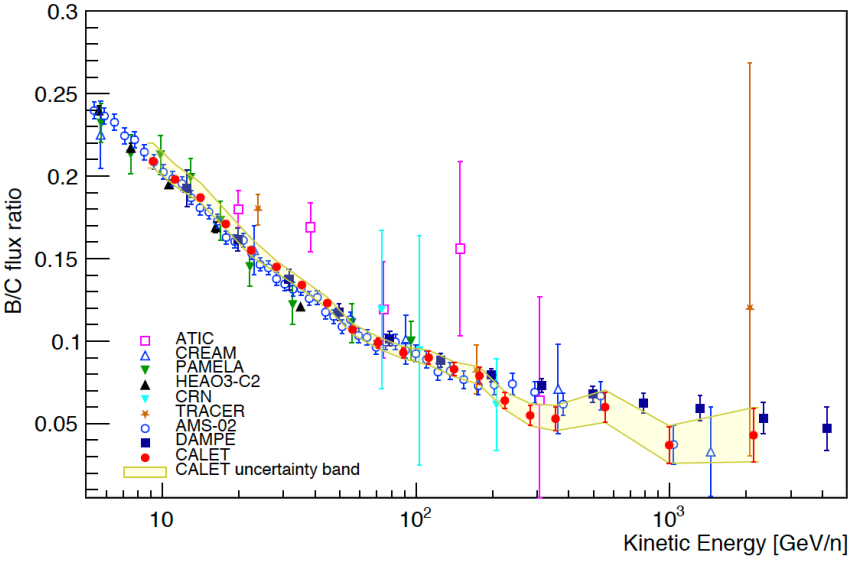

B/O flux ratio

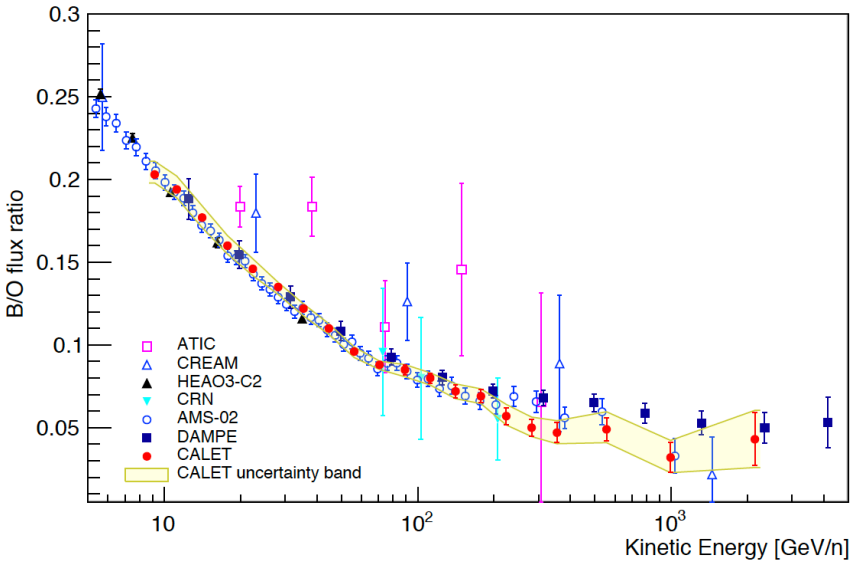

C/O flux ratio

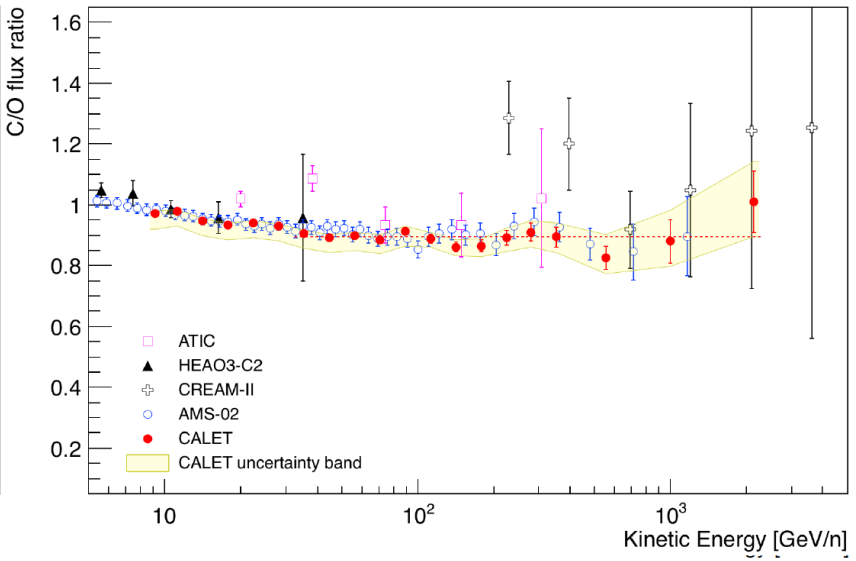

- Flux ratios of B/C and B/O are in agreement with AMS02 and lower than DAMPE result above 300 GeV/n, although consistent within the error bars.
- C/O flux ratio as a function of energy is in good agreement with AMS-02.
- At E > 30 GeV/n the C/O ratio is well fitted to a constant value 0.90 ± 0.03 with $\chi^2/\mathrm{dof} = 8.1/13$.
  ⇨ C and O fluxes have the same energy dependence.
- At E < 30 GeV/n C/O ratio is slightly softer.
  ⇨ secondary C from O and heavier nuclei spallation

Spectral Fit of B/C and B/O

PRL 125 251102 (2020) + CRD4-04

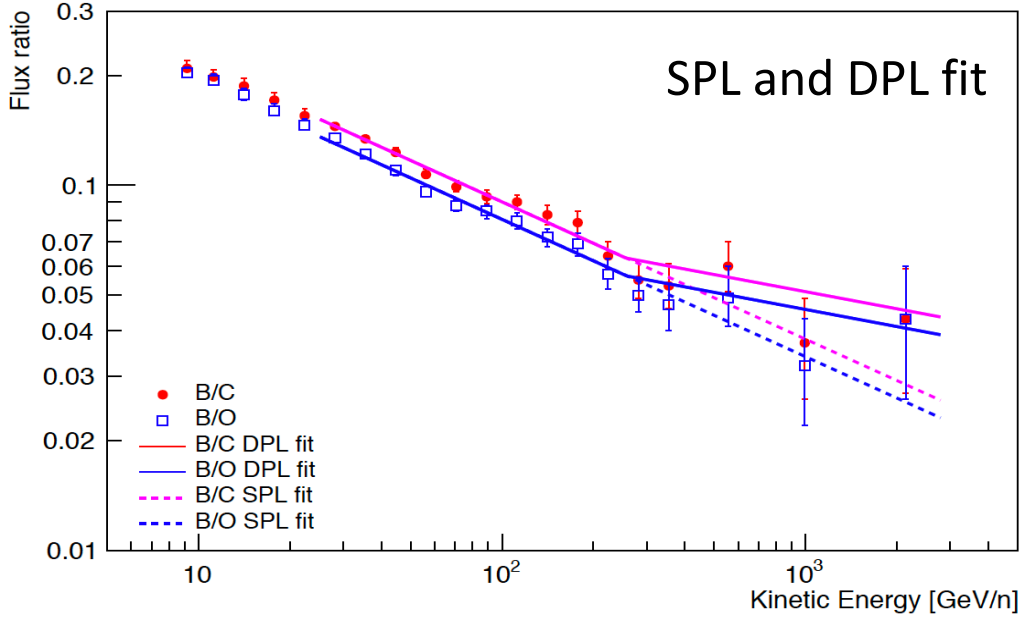

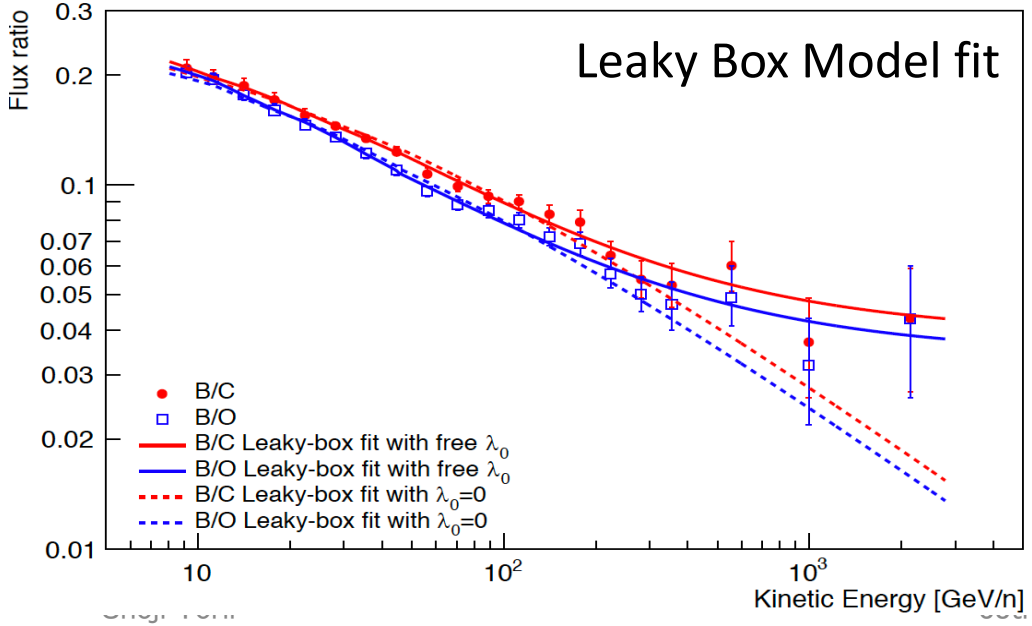

Simultaneous fit to B/C and B/O (E>25 GeV/n) with same parameters except normalization

SPL fit	$\Gamma = -0.376 \pm 0.014$	(χ^2/dof = 19/27)
DPL fit	$\Delta\Gamma = 0.22 \pm 0.10$	(χ^2/dof = 15/26)

Leaky-box model fit [ApJ **752** 69 (2012)]

$$\frac{\Phi_B(E)}{\Phi_C(E)} = \frac{\lambda(E)\lambda_B}{\lambda(E)+\lambda_B}\left[\frac{1}{\lambda_{C\to B}} + \frac{\Phi_O(E)}{\Phi_C(E)}\frac{1}{\lambda_{O\to B}}\right] \quad \frac{\Phi_B(E)}{\Phi_O(E)} = \frac{\lambda(E)\lambda_B}{\lambda(E)+\lambda_B}\left[\frac{1}{\lambda_{O\to B}} + \frac{\Phi_C(E)}{\Phi_O(E)}\frac{1}{\lambda_{C\to B}}\right]$$

$\lambda(E)$: mean escape path length

$\lambda(E) = kE^{-\delta} + \lambda_0$

λ_0 : residual path length

δ : diffusion coefficient spectral index

See details of assumption in CRD4-04 by Paolo Maestro

Fit parameters	λ_0 =0 fixed	λ_0 free
k (g/cm^2)	13.1 ± 0.2	13.0 ± 0.3
δ	0.61 ± 0.01	0.81 ± 0.04
λ_0 (g/cm^2)	0	1.17 ± 0.16
χ^2/dof	58.3/38	17.9/37

Significance of $\lambda_0 \neq 0 > 5\sigma$ ⇨ Residual path length could explain the flattening of B/C, B/O ratios at high energies.

Flux Ratio between Light Nuclei Primary Elements

CRD2-02

C/He and O/He ratio with constant fitting

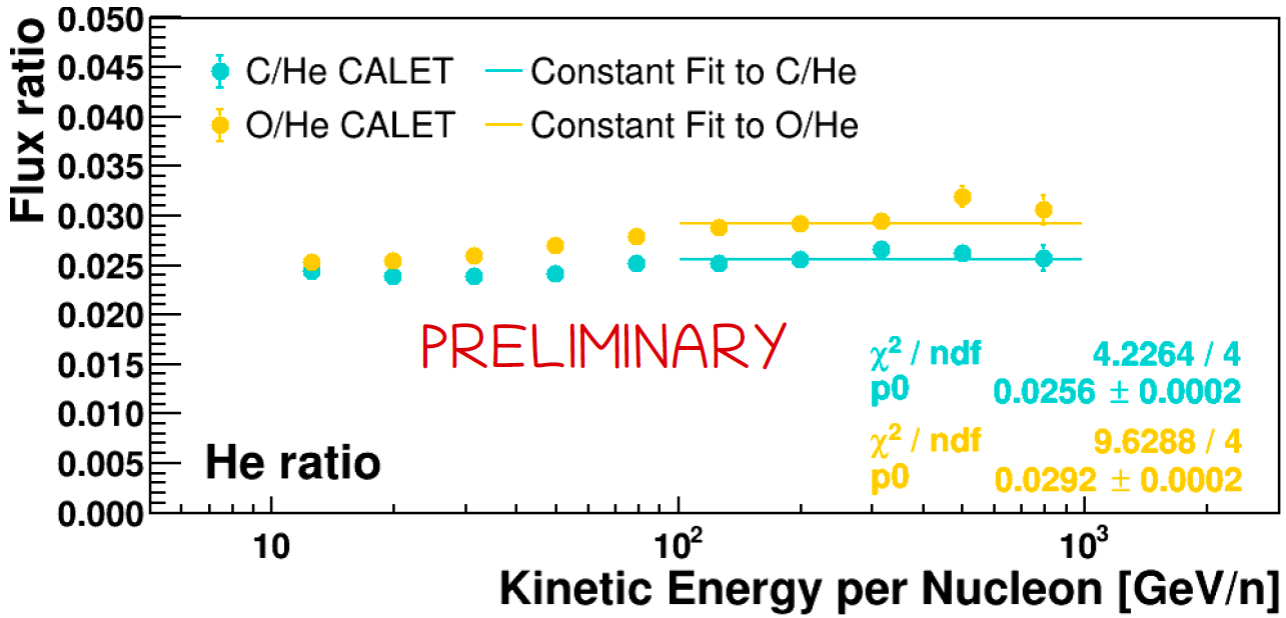

O/C ratio with constant fitting

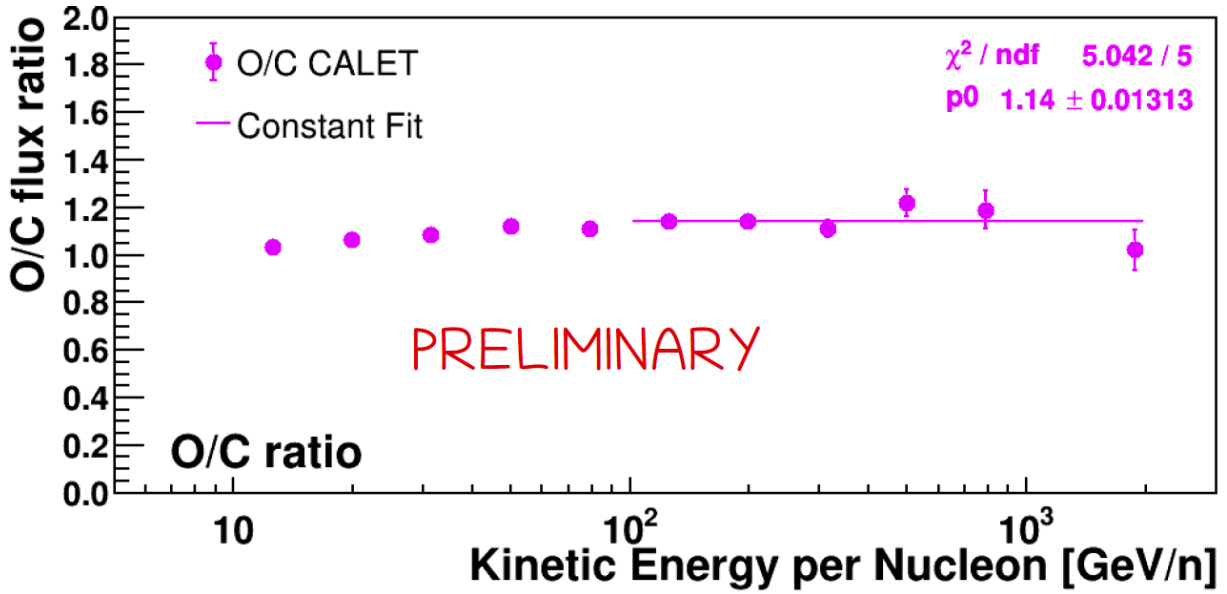

The flux ratio between light nuclei (He, C, O) is constant above 100 GeV/n.

Iron Energy Spectrum

PRL 126 241101 (2022) + CRD2-05

Flux x $E^{2.6}$ vs kinetic energy per nucleon (Nov.2016-Dec.2022)

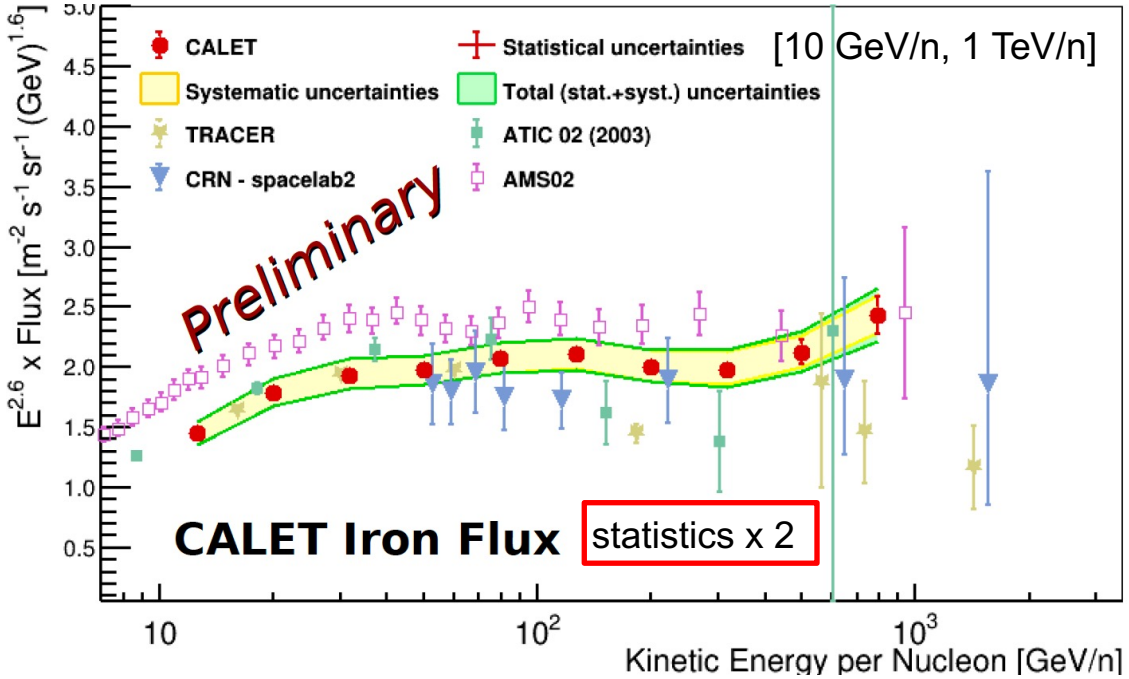

Fit from 50 to 800 GeV/n, with SPL & DPL

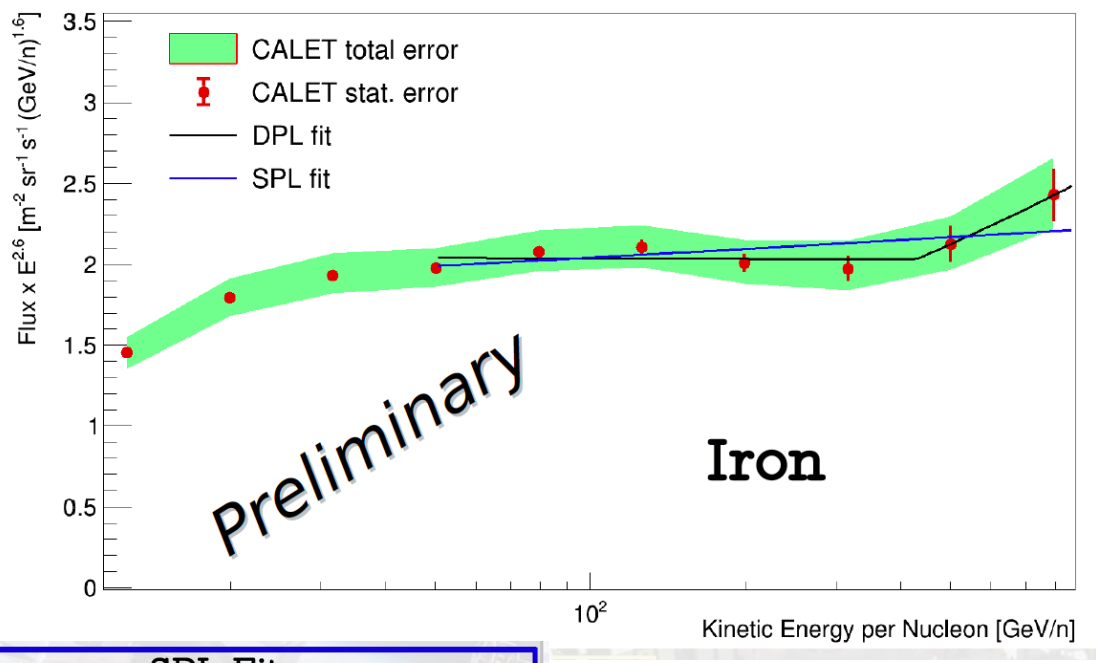

Low energy (< 10 GeV) measurement using geomagnetic cut-off (Oct. 2015 to May 2021)

PCRD0-25

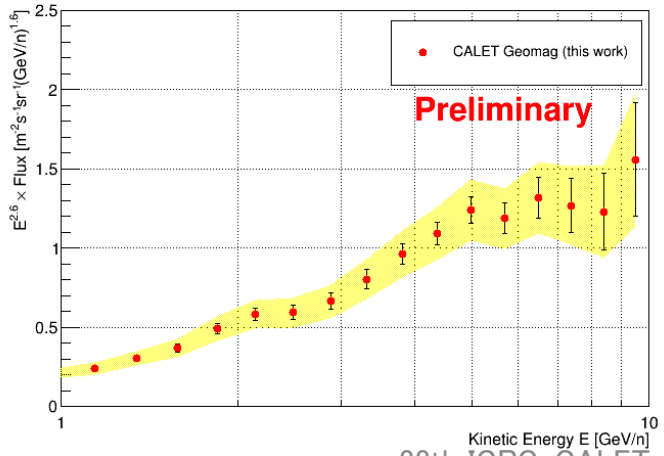

SPL Fit

$$\Phi(E) = C\left(\frac{E}{1\ \mathrm{GeV}}\right)^{\gamma}$$

- $\gamma = -2.56 \pm 0.01(\mathrm{stat}) \pm 0.03(\mathrm{sys})$
- $\chi^2/\mathrm{DOF} = 2.7/5$

DPL Fit

$$\Phi(E) = \begin{cases} c\left(\frac{E}{\mathrm{GeV}}\right)^{\gamma} & E \le E_0 \\ c\left(\frac{E}{\mathrm{GeV}}\right)^{\gamma}\left(\frac{E}{E_0}\right)^{\Delta\gamma} & E > E_0 \end{cases}$$

- $\gamma = -2.60 \pm 0.01(\mathrm{stat}) \pm 0.08(\mathrm{sys})$
- $\chi^2/\mathrm{DOF} = 0.8/3$
- $\Delta\gamma = 0.29 \pm 0.27$
- $E_0 = (428 \pm 314)$ Gev/n

The significance of the fit with the DPL in the studied energy range is not sufficient to exclude the possibility of a single power law

Nickel Energy Spectrum

PRL 128 131103 (2022) + CRD2-05

Flux x $E^{2.6}$ vs kinetic energy per nucleon

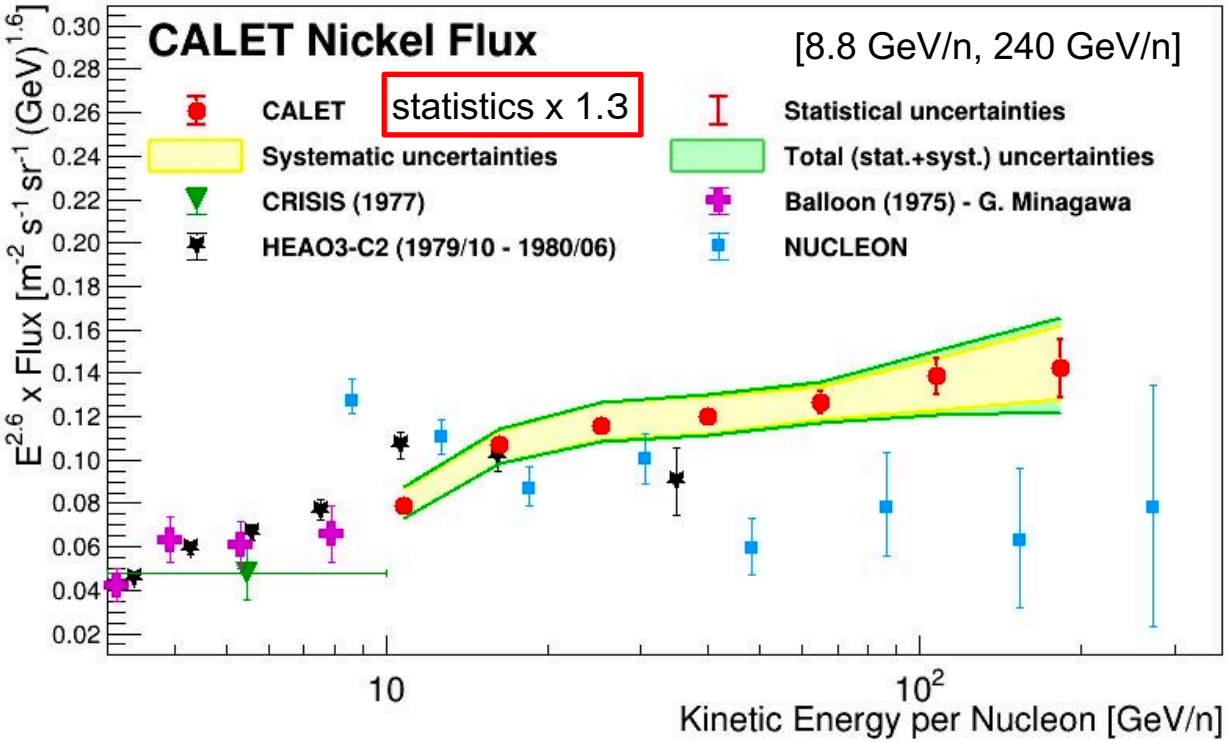

Fit from 20 to 240 GeV/n, with a SPL

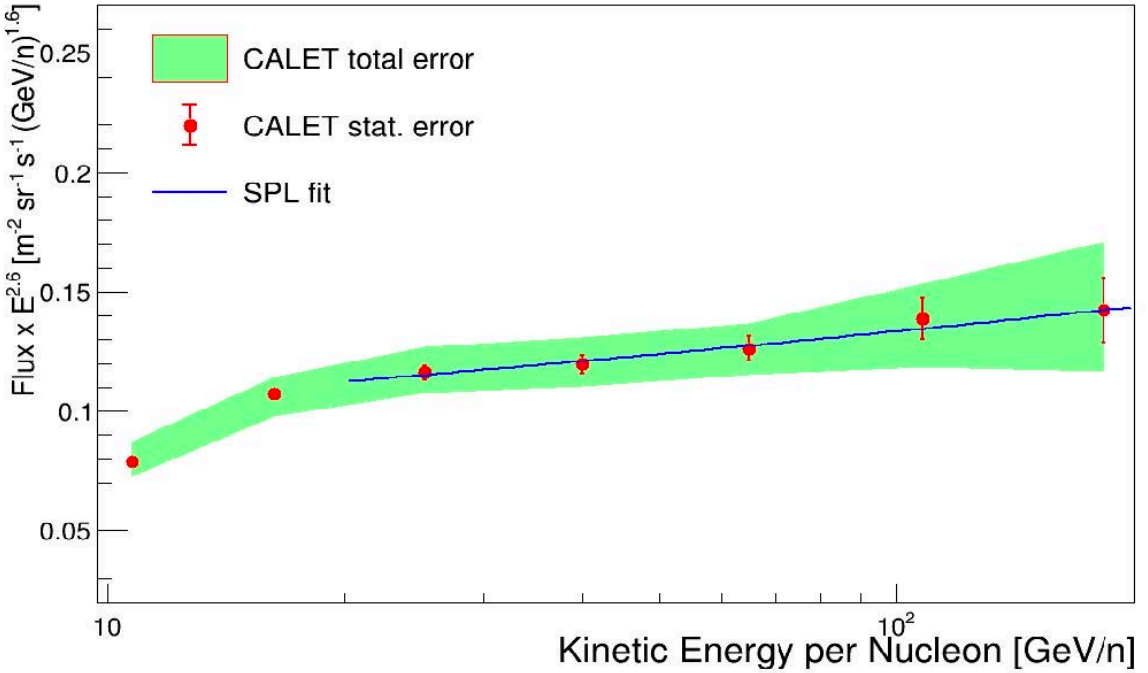

Charge separation between Fe and Ni

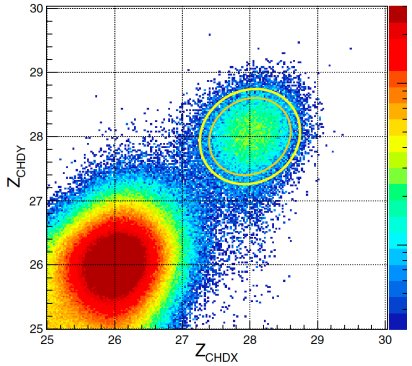

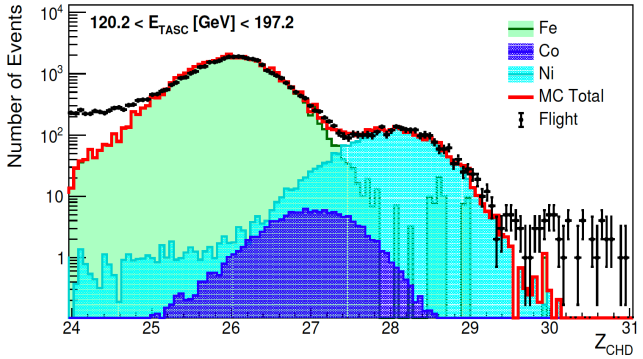

SPL Fit

$$\Phi(E) = C\left(\frac{E}{1\ \mathrm{GeV}}\right)^{\gamma}$$

- $\gamma = -2.49 \pm 0.03(\mathrm{stat}) \pm 0.07(\mathrm{sys})$
- $\chi^2/\mathrm{DOF} = 0.1/3$

From 20 to 240 GeV/n the nickel flux is consistent with the hypothesis of an SPL Spectrum.

Flux Ratios of Iron to Primary Elements

CRD2-02

Fe ratios to He, C and O

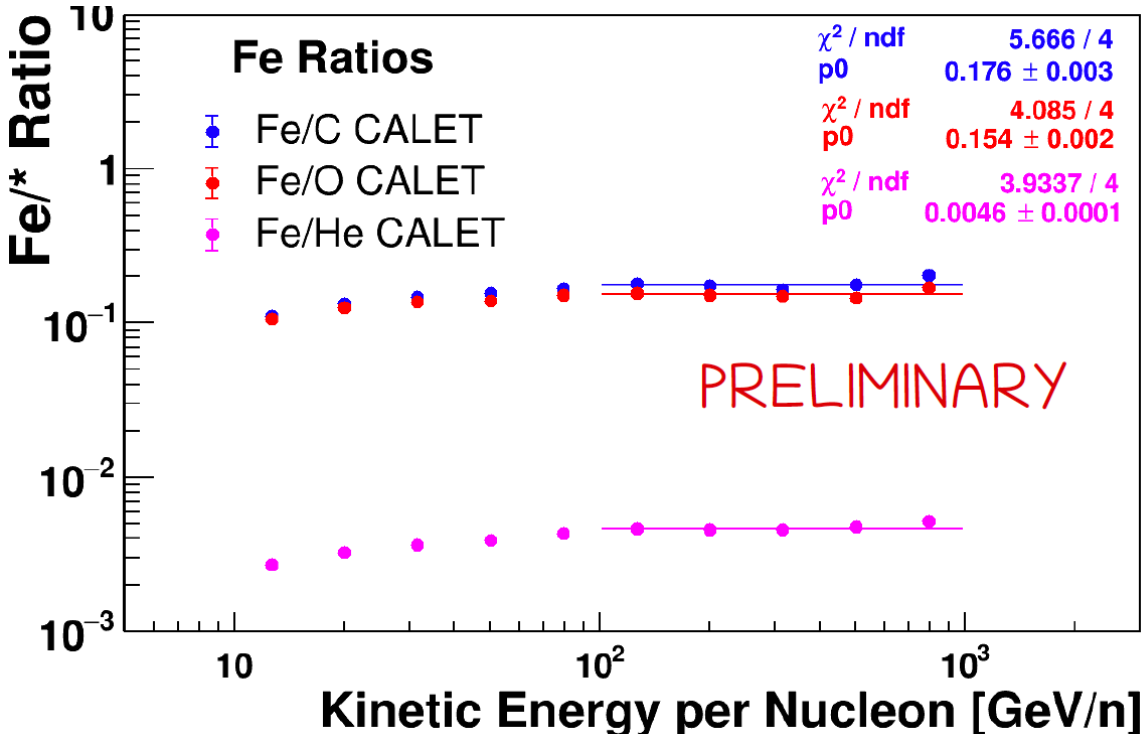

Fe ratios to He, C and O normalized at 100 GeV/n

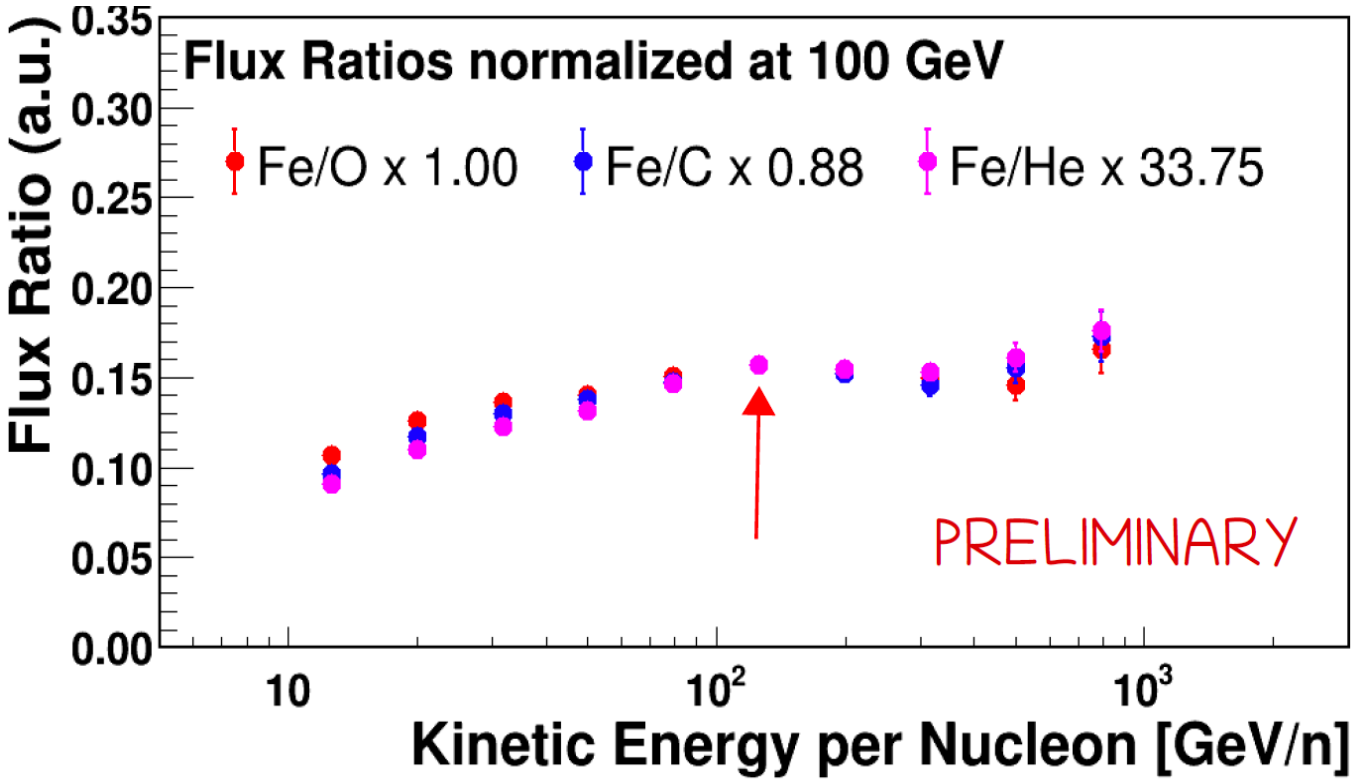

Fe/O, Fe/C and Fe/He are compatible with a constant above 100 GeV/n within errors.
⇨ Fe, O, C follow similar propagation

Flux Ratios of Nickel to Primary Elements

CRD2-02

Ni ratios to He, C, O and Fe

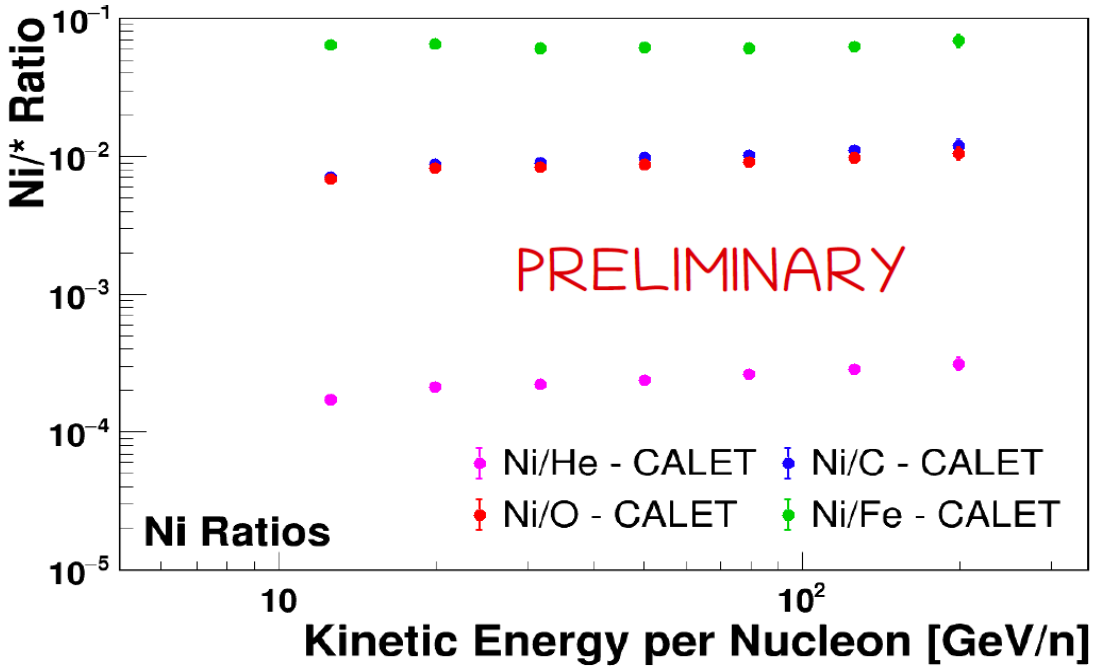

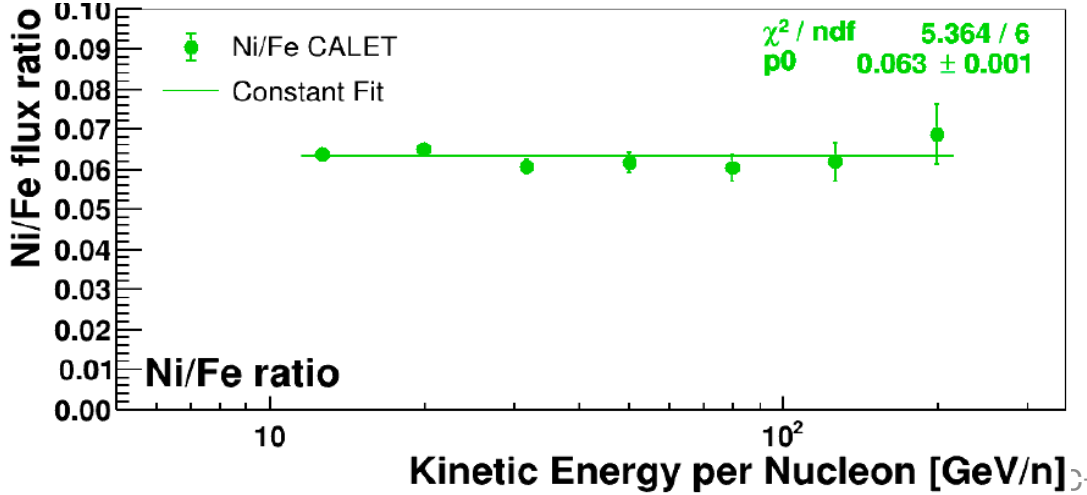

Ni ratios normalized at around 10 GeV/n

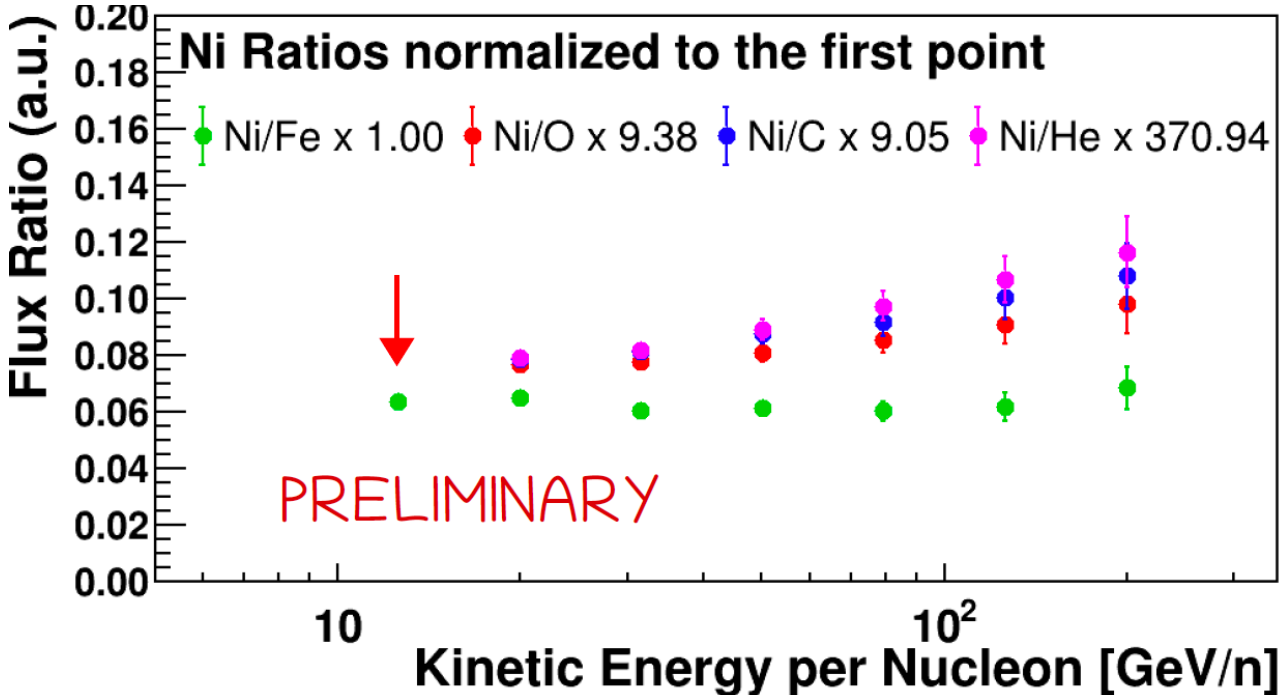

- The Ni/Fe flux ratio is constant in all the energy range thus Ni and Fe have very similar behavior.
- The present energy range of nickel flux does not allow to fit the Ni/* ratios with a constant above 100 GeV/n.
- At low energy the Ni/O, Ni/C, Ni/He flux ratio show an increasing trend also visible in Fe/* ratios.

Ultra-heavy Cosmic-ray Nuclei (26 < Z ≤ 44)

CRD3-06 + PCRD11-15

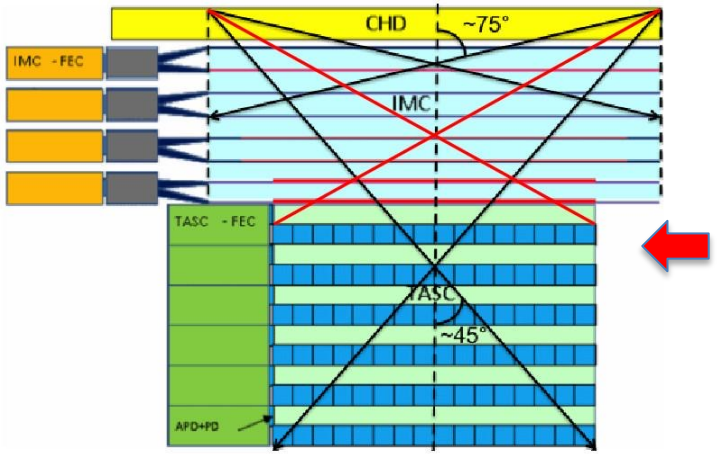

- A special UH CR trigger uses the CHD and the first 4 layers of the IMC to achieve an expanded x 4 geometric factor **GF ~ 4400 cm^2 sr** without energy information.
  (~260 million events)
- A subset of events pass through the top of the TASC (~65 million events) with energy information,

Charge histogram

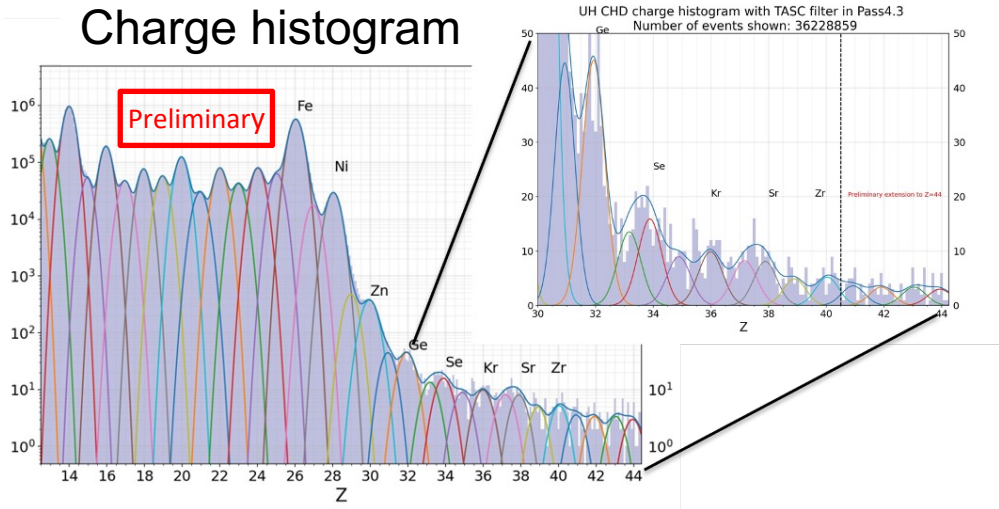

Mesurement of the relative abundances of the elements above Fe through $_{44}$Ru (Fe =1)

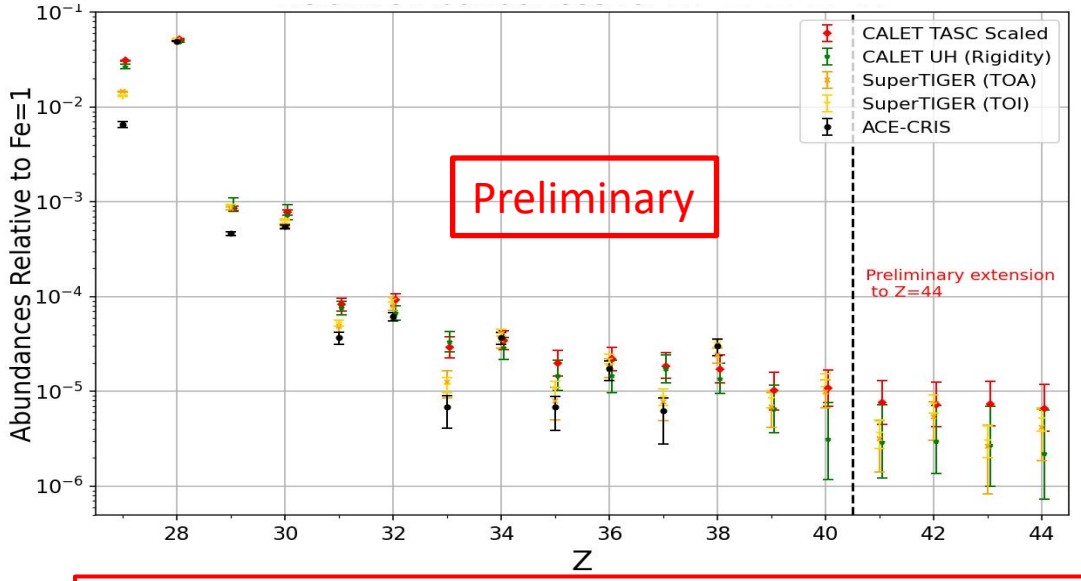

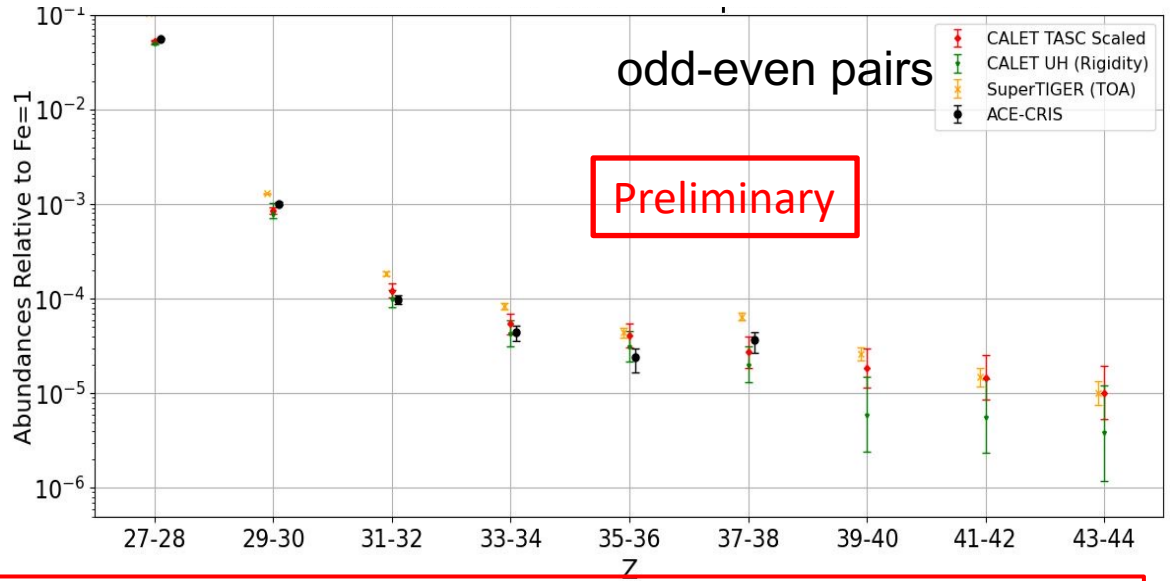

The CALET UH element ratios relative to Fe are consistent with Super-TIGER and ACE abundances.

CALET γ–ray Sky Map and Energy Spectra

GA17-06 + PGA2-10

- Effective area: ~400 cm^2 (>2 GeV)
- Angular resolution: < 0.2° (> 10 GeV)
- Energy resolution: ~2% (> 10 GeV)

Gamma-ray sky map LE-γ trigger (E >1 GeV)

Gamma-ray sky map HE trigger (E>10 GeV)

Nov. 2015 – Dec. 2022

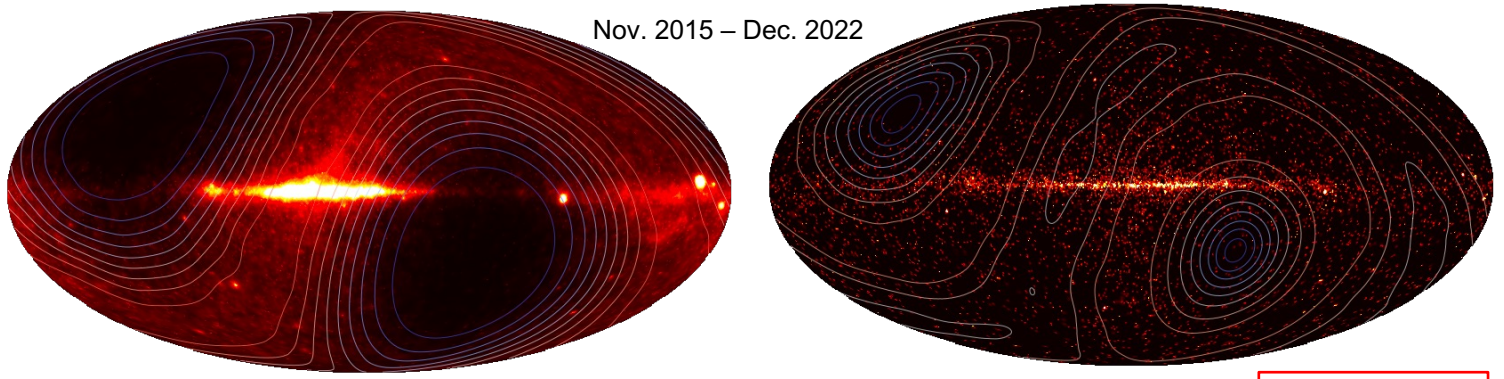

Energy spectra for bright point sources

Preliminary

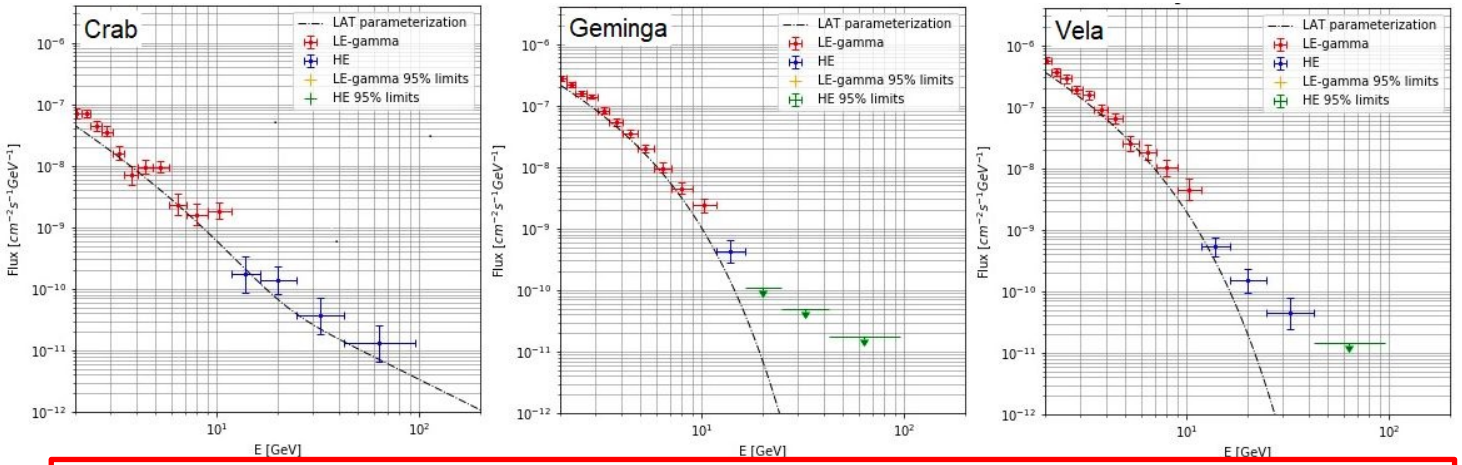

The spectra for point sources and diffuse components are found to be consistent with those by Fermi-LAT .

Gamma-ray spectrum

Preliminary

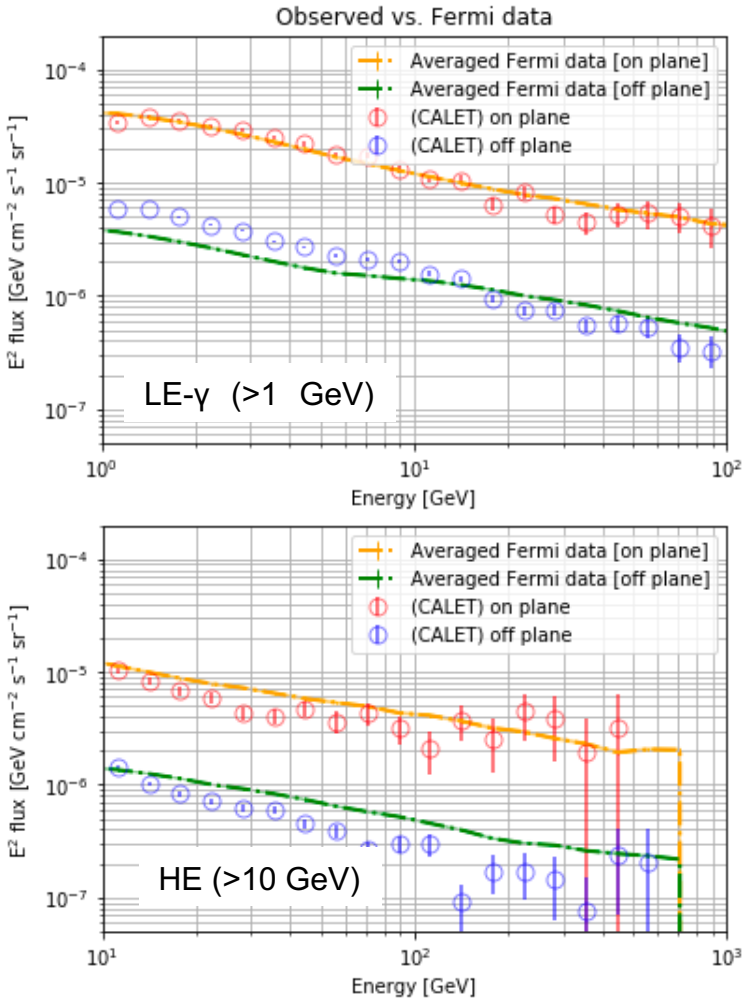

"On-plane": $|l| < 80°$ & $|b| < 8°$, "Off-plane": $|b| > 10°$

Gamma-ray Bursts and GW Follow-up

ApJ 933:85 (2022) + PMM GW3-17

CGBM Specifications

	HXM	SGM
Crystal	LaBr3(Ce)	BGO
Number of detectors	2	1
Diameter [mm]	66.1 (small) 78.7 (large)	102
Thickness [mm]	12.7	76
Energy range [keV]	7-1000	40-20000
Field of view	~3 sr	~8 sr

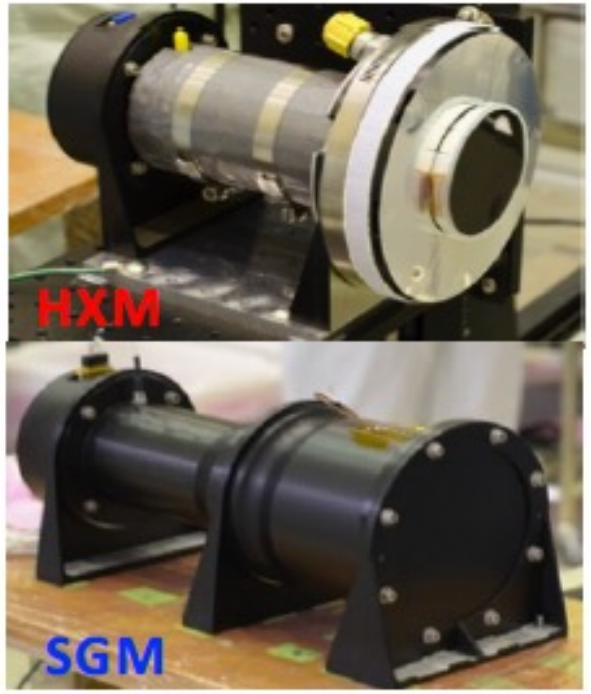

- **Follow-up** of LIGO/Virgo **GW** observations during O3 & O4
- X-ray and gamma-ray bands
- High-energy gamma-ray in the calorimeter

CGBM has detected 327 GRBs as of June 2023.

Duration distribution measured by SGM (40 – 1000 keV)

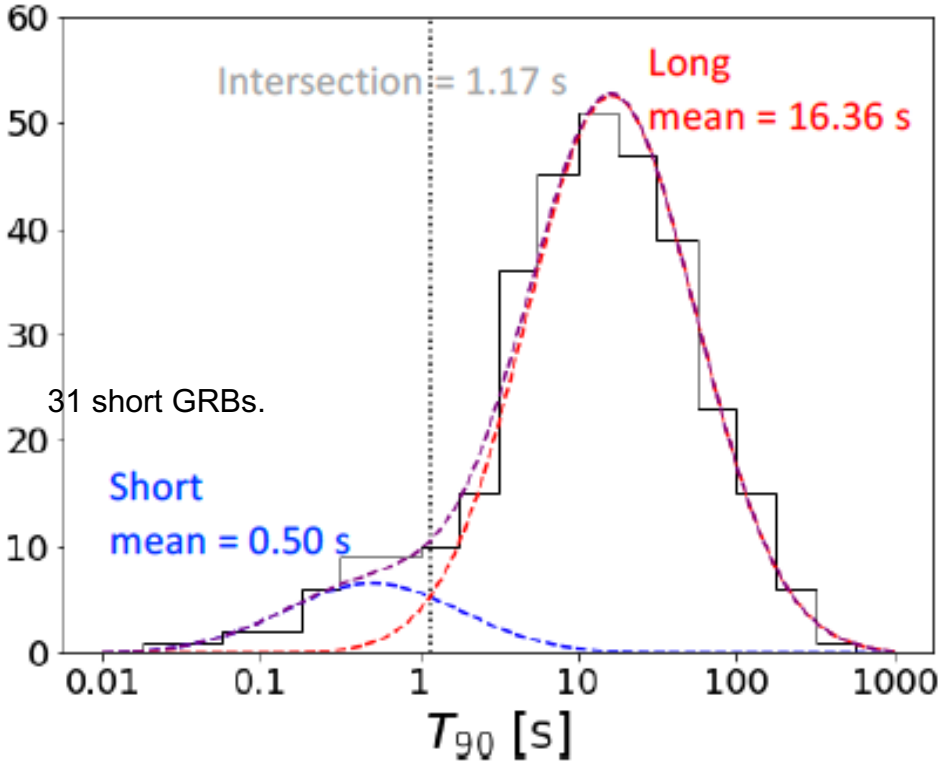

- We developed **automatic pipelines to process CGBM and CAL data** to analyze O4 events with higher event rates.
- **169 events have been reported via GCN Notice** in ER15 and O4, and the developed pipelines have been **triggered by LVC NOTICE and processed CALET data**, and enabled us to check many GW events.

Solar Modulation and Drift Model

PRL 130 211001 (2023) + PSH3-05

Solar Modulation during Solar Cycles 24-25 Transition

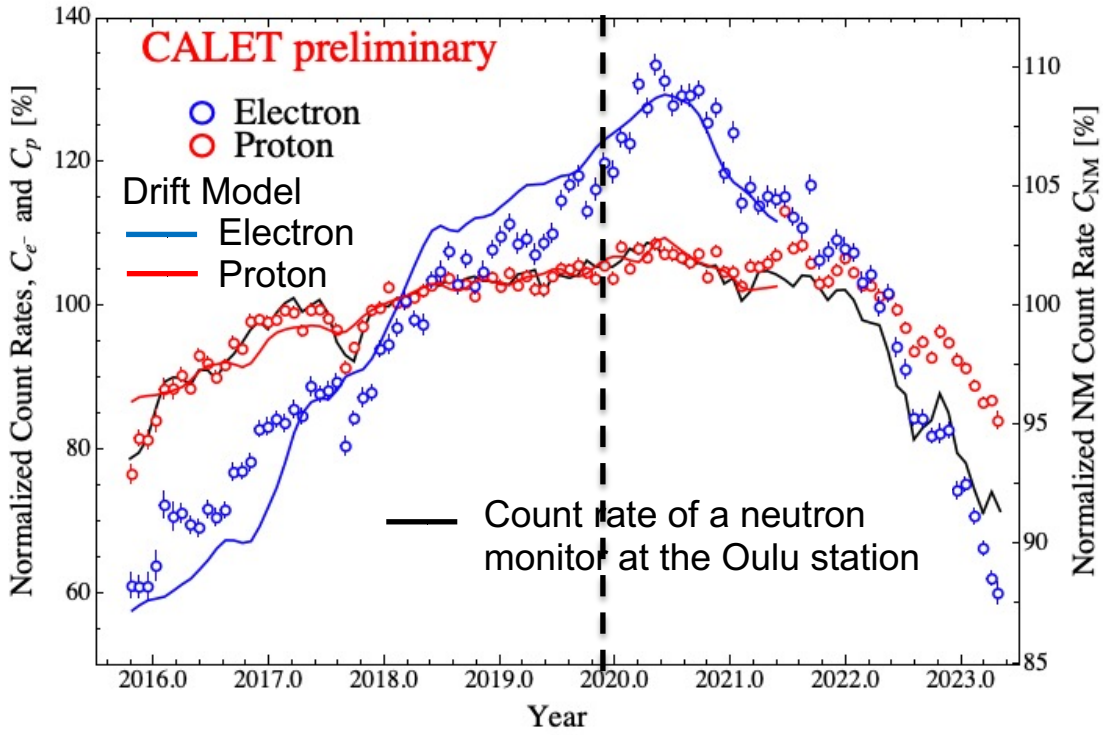

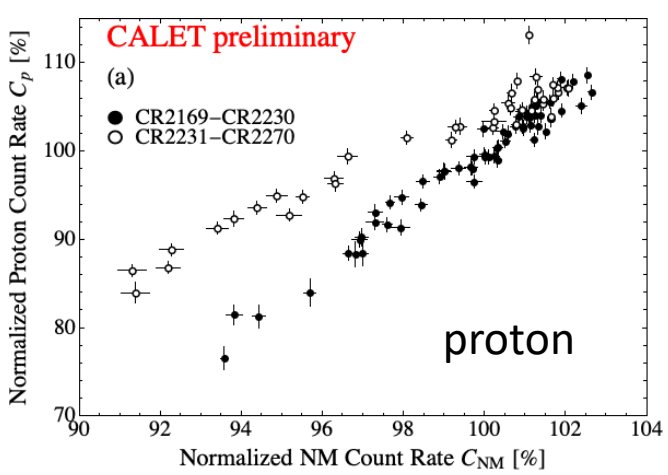

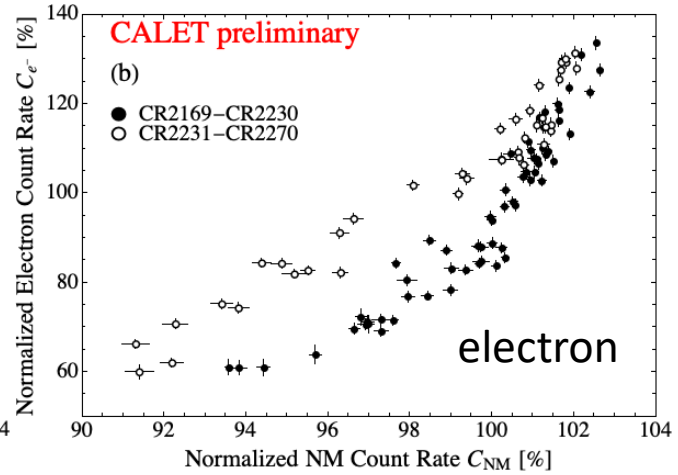

CALET proton (a) and electron (b) count rates at the average rigidity of 3.8 GV as a function of neutron monitor count rates at the Oulu station during the descending phase in the 24th solar cycle (closed circles) and the ascending phase in the 25th solar cycle (open circles).

- We have observed a clear charge-sign dependence of the solar modulation of GCRs, showing that variation amplitude of C_{e-} is much larger than that of C_p at the same average rigidity.
- We also have succeeded in reproducing variations of C_{e-} and C_p simultaneously with a numerical drift model of the solar modulation, which implies that the drift effect plays a major role in the long-term modulation of GCRs.
- We also find a clear difference between ratios, C_p/C_{NM}, during the descending phase of the 24th solar cycle and the ascending phase of the 25th solar cycle.

Space Weather Phenomena with CALET

GRL 49 (2022) + PCRD3-14

- To identify relativistic electron precipitation (REP) in the CALET dataset an algorithm was developed which use self organizing maps (SOM), an unsupervised machine learning technique, to both detect and categorize potential REP events.
- For a period from October 2015 to October 2021 this method found a total of 1448 rapid REP events and 21301 smooth profile events.

Relativistic Electron Precipitation (REP) Events with CALET

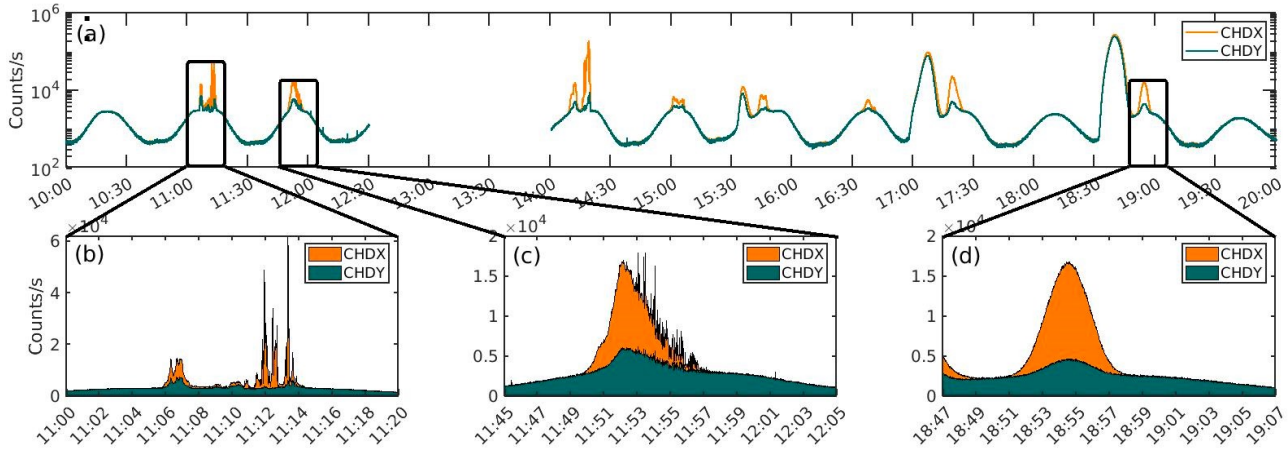

rapid mixed between rapid and smooth smooth

CALET and Radiation Belt Science Probes (RBSP)

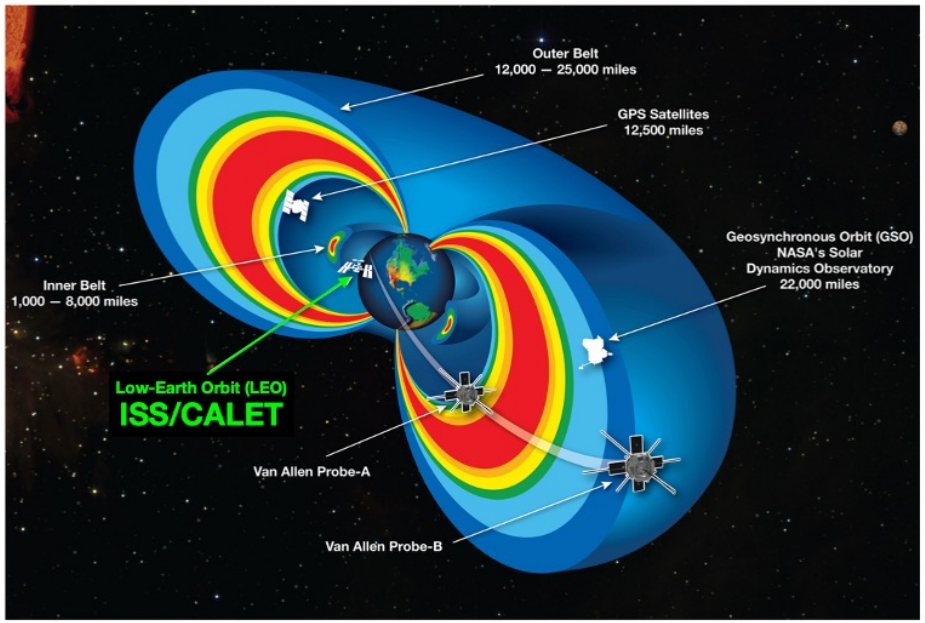

- 664 events were identified in RBSP-A data and 443 events for RBSP-B

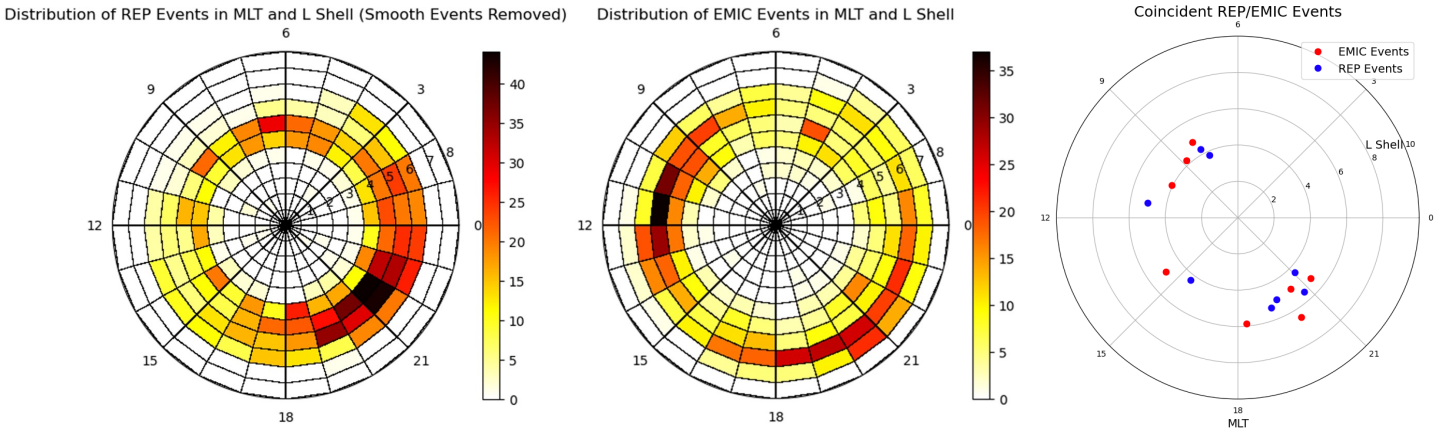

Spatial distribution in terms of magnetic local time (MLT) and L shell for observed REP events (left) and observed EMIC wave events (right).

Spatial distribution of coincident REP/EMIC wave events in MLT and L.

Summary and Future Prospects

CALET was successfully launched in August 2015 and installed on the JEM-EF module on the ISS

- Operational over 2800 days with 86% live time, total triggers approaching 4 billion

Continuous on-orbit updates from ground calibration	Astropart. Phys. 91, 1 – 10 (2017)
Stable operations over a range of observing modes continue	Astropart. Phys. 100, 29 – 37 (2018)

- Analysis of CR events continues, extending to higher energies and charges

All-electron spectrum in the range 11 GeV – 4.8 TeV	PRL 120, 261102 (2018)	(2nd update)
Proton spectrum in the range 50 GeV – 60 TeV	PRL 129, 101102 (2022)	(2nd update)
Carbon and oxygen spectra in the range 10 GeV/n – 2.2 TeV/n	PRL 125, 251102 (2020)	1st paper
Iron spectrum in the range 50 GeV/n – 2 TeV/n	PRL 126, 241101 (2021)	1st paper
Nickel spectrum in the range 8.8 GeV/n – 240 GeV/n	PRL 128, 131103 (2022)	1st paper
Boron spectrum in the range 8.4 GeV/n – 3.8 TeV/n	PRL 129, 251103 (2022)	new
Helium spectrum in the range 40 GeV – 250 TeV	PRL 130, 171002 (2023)	new
Preliminary analysis of ultra-heavy cosmic-ray abundances	see W.Zober CRD3-06 (ICRC2023)	preliminary

- Analysis of gamma-ray sources and transients continues

Calorimeter instrument response characterized	ApJS 238:5 (2018)
GW follow-up and GRB analysis with CGBM & CAL	ApJL 829:L20 (2016)
Counterpart search in LIGO/Virgo O3 with CGBM & CAL	ApJ 933:85 (2022)

- Analysis of transient heliospheric and space weather phenomena underway

Charge-sign dependence of Solar modulation	PRL 130, 211001 (2023)	new
Solar energetic particle and relativistic electron precipitation events	see A.Ficklin PCRD2-14(ICRC2023)	

Extended operations approved by JAXA/NASA/ASI in March 2021 through the end of 2024 (at least)

List of CALET Talks at ICRC2023 +12 Posters

ID	Presenter	Title	Date
CRD5-02	Y. Akaike	Energy spectrum of cosmic-ray electron and positron measured with CALTE on the International Space Station	July 29
CRD1-01	K. Kobayashi	Observation of spectral structures in the flux of cosmic ray protons with CALET on the International Space Station	July 26
CRD1-02	P. Brogi	Helium flux and its ratio to proton flux in cosmic rays measured with CALET on the International Space Station	July 26
CRD4-04	P. Maestro	Boron flux in cosmic rays and its flux ratio to primary species measured with CALET on the International Space Station	July 28
CRD2-05	F. Stolzi	Iron and Nickel fluxes measured by CALET on the International Space Station	July 27
CRD2-02	C. Checchia	Flux ratios of primary elements measured by CALET on the International Space Station	July 27
CRD3-06	W. Zober	Results of the Ultra-Heavy Cosmic-Ray Analysis with CALET on the International Space Station	July 27
GA17-06	M. Mori	Results from CALorimetric Electron Telescope (CALET) Observations of Gamma-rays	July 31
DM5-03	H. Motz	Dark Matter Limits from the CALET Electron+Positron Spectrum with Individual Astrophysical Source Background	Aug. 2

Thank you for your attention

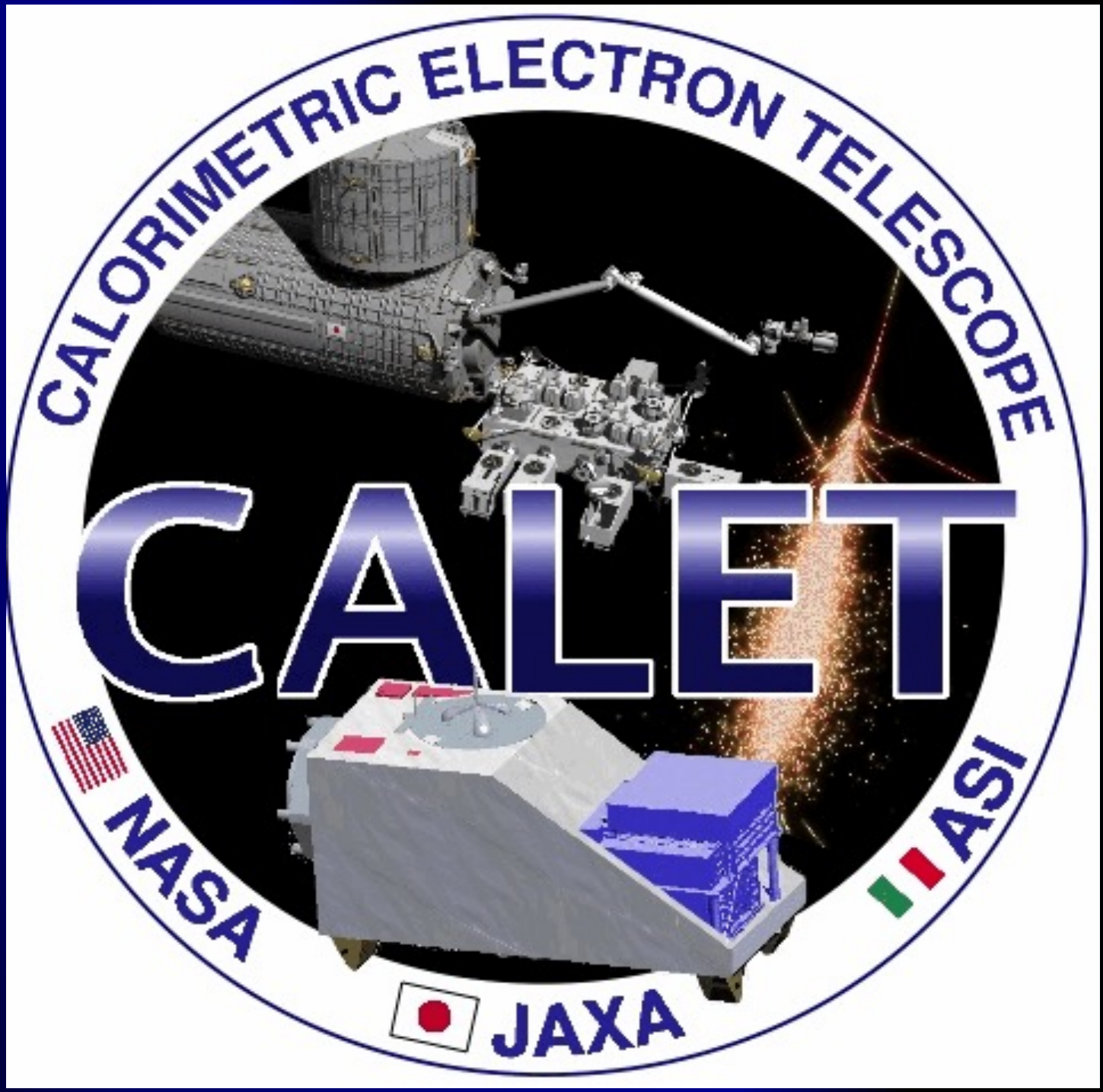

Towards an Interpretation of the CALET All-electron Spectrum

Preliminary results using ICRC2021 data are presented for :

- Interpretation of the electron + positron spectrum by astrophysical sources at PCRD2-07
- Dark Matter limits with individual astrophysical source background at DM5-03

An example of Dark Matter limits in annihilation

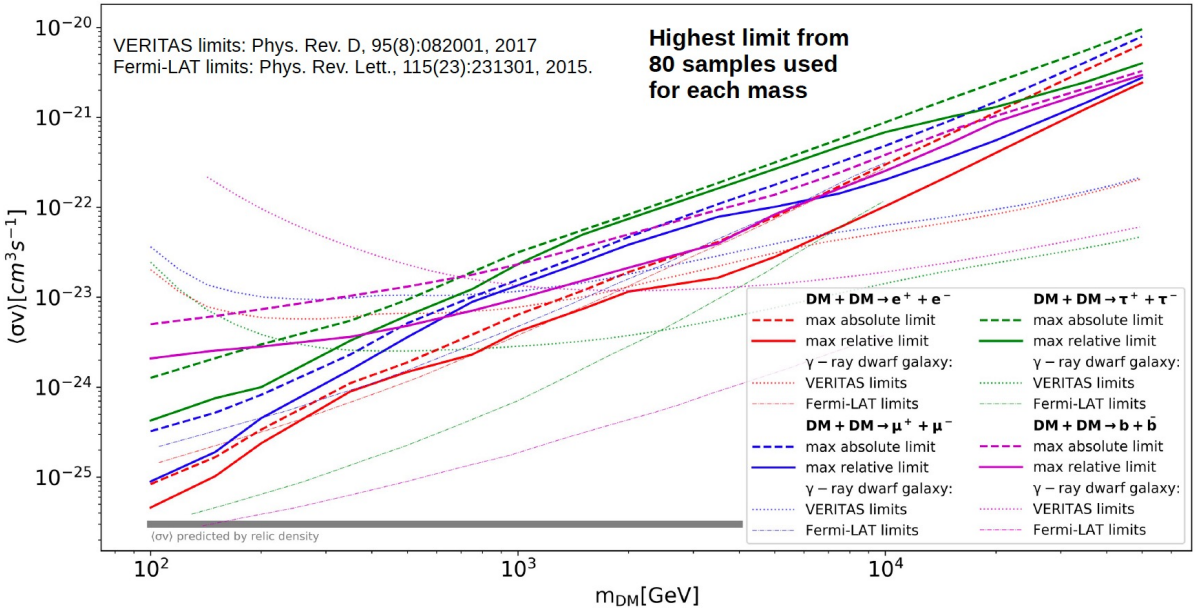

An example of fit by astrophysical sources (pulsar & SNR)

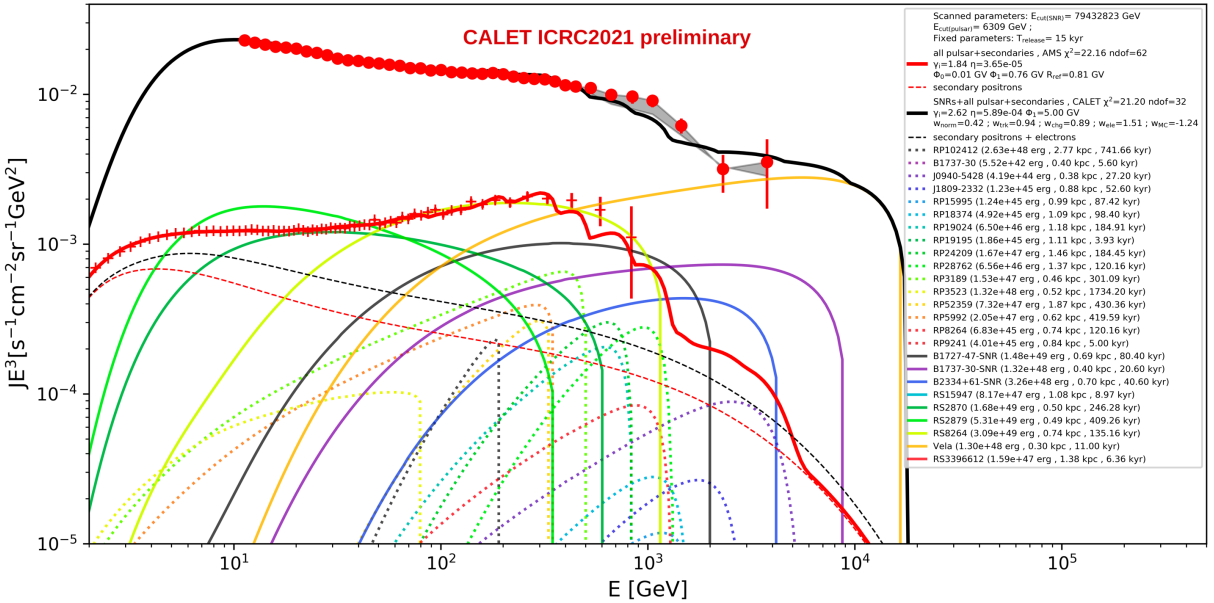

See the details in the presentations